

pubs.acs.org/JCTC Article

The Harmonic and Gaussian Approximations in the Potential Energy Landscape Formalism for Quantum Liquids

Yang Zhou,* Gustavo E. Lopez,* and Nicolas Giovambattista*



Cite This: https://doi.org/10.1021/acs.jctc.3c01085



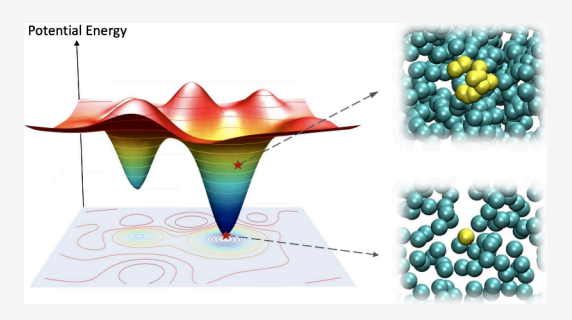
ACCESS I

III Metrics & More

Article Recommendations

Supporting Information

ABSTRACT: The potential energy landscape (PEL) formalism has been used in the past to describe the behavior of classical low-temperature liquids and glasses. Here, we extend the PEL formalism to describe the behavior of liquids and glasses that obey quantum mechanics. In particular, we focus on the (i) harmonic and (ii) Gaussian approximations of the PEL, which have been commonly used to describe classical systems, and show how these approximations can be applied to quantum liquids/glasses. Contrary to the case of classical liquids/glasses, the PEL of quantum liquids is temperature-dependent, and hence, the main expressions resulting from approximations (i) and (ii) depend on the nature (classical vs quantum) of the system. The resulting theoretical expressions from the PEL formalism are compared with



results from path-integral Monte Carlo (PIMC) simulations of a monatomic model liquid. In the PIMC simulations, every atom of the quantum liquid is represented by a ring-polymer. Our PIMC simulations show that at the local minima of the PEL (inherent structures, or IS), sampled over a wide range of temperatures and volumes, the ring-polymers are collapsed. This considerably facilitates the description of quantum liquids using the PEL formalism. Specifically, the normal modes of the ring-polymer system/quantum liquid at an IS can be calculated analytically if the normal modes of the classical liquid counterpart are known (as obtained, e.g., from classical MC or molecular dynamics simulations of the corresponding atomic liquid).

1. INTRODUCTION

Understanding the behavior of liquids at low temperatures, close to their glass transition temperature, and understanding the nature of the associated glass state have been fundamental issues in material science for many decades. ^{1–7} Numerous theoretical/computational approaches have been proposed to address these issues. ^{3,7–11} In most of these approaches, the focus is on *classical* liquids and glasses, where nuclear quantum effects (NQEs) are neglected. While this is justified in the case of high-temperature glass-formers, such as silica, the role of atom delocalizations due to NQEs cannot be ignored in substances composed of light elements, such as H₂ and He, as well as in liquids/glasses composed of small molecules containing H, including water. ^{12,13} The case of water is a clear example since computer simulations show that NQE can alter the thermodynamic properties of crystalline and amorphous ice (glassy water) at cryogenic temperatures. ¹⁴

A particularly successful theoretical/computational approach to describe liquids and glasses is the potential energy landscape (PEL) formalism. The PEL formalism is based on statistical mechanics and, in its original formulation, the is limited to classical liquids/glasses. However, as we explain in ref 22, the PEL formalism can be extended to the case of quantum liquids/glasses by using the path-integral formulation of statistical mechanics. As explained in detail below, the basic idea of this approach is to apply the PEL formalism to the PEL defined by the ring-polymers that represent the atoms in the

system. In principle, the ring-polymer system PEL (RP-PEL) can be used to extract thermodynamic properties of the quantum liquid/glass of interest (with NQE included).²² A few years ago, the concept of RP-PEL [or, path-integral (potential) energy landscape] was applied to study a small cluster of water molecules.²³ However, ref 23 focused on the characterization of the transition states of the system. The extension of the PEL formalism to study the thermodynamic properties of quantum systems, including liquids/glasses, is not yet well understood.²² Interestingly, the relevance of extending the PEL formalism to study quantum liquids/glasses was already noticed by Stillinger approximately 35 years ago.²⁴ However, probably due to the limited computational resources at the time, the PEL formalism to study quantum liquids/glasses was not developed in ref 24

In this work, we build upon our previous study²² and further develop the PEL formalism to the case of liquids/glasses that obey quantum mechanics. We first provide the mathematical background necessary to understand how the PEL can be

Received: September 30, 2023 Revised: December 11, 2023 Accepted: January 3, 2024



combined with the path-integral formulation of statistical mechanics to study quantum systems, including liquid/glasses, Section 3.1. In particular, we also extend the (i) harmonic approximation and (ii) revisit the Gaussian approximation of the PEL. Approximations (i) and (ii) have been used extensively in the past to study classical liquids and make the PEL formalism of practical use. For example, with these approximations, the PEL formalism has been used to obtain the thermodynamic and dynamical properties of liquids, including silica²⁵ and water.²⁶ In ref 22 we performed pathintegral Monte Carlo simulations of an atomistic model liquid (Fermi-Jagla model, FJ) and found that, curiously, the ringpolymers representing the atoms of the liquid collapsed after potential energy minimization, i.e., at the local minima of the PEL (inherent structures, IS). In this work, we extend these calculations to include a wide range of volumes and temperatures and find that the collapse of the ring-polymers after minimization of the system potential energy is rather general. As discussed in Section 3.1, this enormously simplifies the application of the harmonic approximation to the case of quantum liquids. For example, as shown in the Appendix, the normal modes of the quantum liquid at the IS sampled by the system can be calculated analytically if the normal modes of the corresponding classical liquid are known. The reported theoretical predictions based on the harmonic and Gaussian approximations of the PEL for quantum liquids are also tested using path-integral Monte Carlo simulations of the FJ liquid (Section 3.2).

2. COMPUTATIONAL METHODS

We perform path-integral Monte Carlo (PIMC) simulations of a monatomic liquid with isotropic pair interactions given by the Fermi–Jagla (FJ) potential. The FJ potential is characterized by a core-softened part and two length-scales, a hard-core radius $r \approx a$, and an attractive minimum at r = b = 1.97a; see Figure 1. Specifically,

$$U(r) = \epsilon_0 \left[\frac{a^n}{r^n} + \frac{A_0}{1 + \exp\left[\frac{A_1}{A_0}(r/a - A_2)\right]} - \frac{B_0}{1 + \exp\left[\frac{B_1}{B_0}(r/a - B_2)\right]} \right]$$
(1)

The parameters A_i and B_i (i = 0, 1, 2) are provided in Table 1 (the parameters ϵ_0 and a are irrelevant since they define, respectively, the units of energy and length). The FJ potential

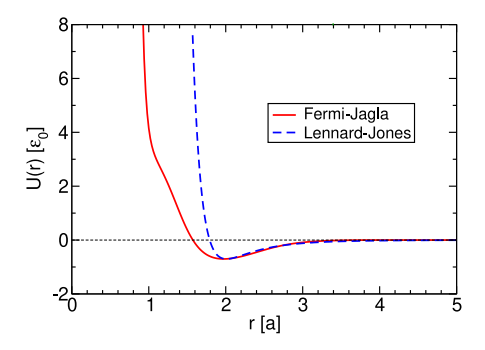


Figure 1. Fermi–Jagla pair interaction potential U(r). The FJ potential is characterized by a hard-core radius $r \approx a$, a core-softened part at approximately $a < r < b \approx 2a$, and a weak attractive part at $r \approx b$. For comparison, we include a Lennard-Jones pair potential with same minimum depth and location as U(r).

Table 1. Pair Interaction Potential Parameters Used in Equation 1; See Figure 1

n	A_0	A_1	A_2	B_0	B_1	B_2
20	4.56	28.88	1.36	1.00	3.57	2.36

is truncated at the cutoff distance $r_c=4.0$ and a switching function is added as implemented in ref 27. The switching function introduces minor modifications in the original FJ potential, at $3.6 \le r \le 4.0$ only, and makes the potential energy and the corresponding forces smooth functions of r (which is suitable for potential energy minimizations). In this work, all properties are given in reduced units by setting the atom mass m=1 and the Boltzmann constant $k_B=1$. Accordingly, the units of energy and distance are, respectively, ϵ_0 and a; the units of T are k_B/ϵ_0 . As a reference, we note that the Lennard-Jones parameters for the case of He atoms are $\epsilon_0\approx 0.085$ kJ/mol and $a\approx 2.28$ Å while, for argon, $\epsilon_0\approx 0.996$ kJ/mol and $a\approx 3.41$ Å (see page 21 in ref 28).

The classical FJ liquid is a model liquid that has been useful in understanding the thermodynamic and dynamic properties of water. Indeed, the FJ liquid exhibits many water-like anomalous properties including the presence of an isothermal compressibility maximum upon isobaric cooling and a diffusivity maximum upon isothermal compression. In addition, as for the case of water, ²⁹ this model liquid exhibits a first-order liquid—liquid phase transition (LLPT) that separates a low-density and high-density liquid state (LDL and HDL) at low temperatures, and glass polymorphism at very low temperatures. In the present study, we mainly focus on PIMC simulations at $\nu = V/N = 2.2$, corresponding to the HDL state; this volume is small enough so that the LLPT does not interfere with our results. ^{30,31}

In order to understand the role of quantum mechanics in the PEL formalism, we follow refs 22 and 31-33 and perform PIMC simulations of the FJ liquid using different values of the Planck's constant h. This allows us to simulate the same liquid in the classical limit (h = 0) as well as in the quantum regime (h > 0). As discussed in Section 3.1.1, the quantum character of the liquid increases with increasing values of h since the atom delocalization becomes more pronounced as h increases. In this study, we consider the cases $h = h_0$, h_1 , h_2 , and h_3 where $h_0 = 0.0000$, $h_1 = 0.2474$, $h_2 = 0.5150$, and $h_3 = 0.7948$, in reduced units of $a(\epsilon_0 m)^{1/2}$. The case $h = h_0$ corresponds to the classical liquid where the ring-polymers are collapsed at all times (for h = 0, the spring constant of the ring-polymers is k_{sp} $\rightarrow \infty$; see below). Hence, for the case $h = h_0$, we perform PIMC simulations where the ring-polymers are composed of one bead.³¹ We note that the values of h > 0 considered here are not negligible. For example, as discussed in detail in ref 22 one obtains h = 1.78 (in reduced units) if the values for (m, a, a, b) ϵ_0) are appropriate to the case of H₂; for argon, $h \approx 0.18$ (in reduced units).2

Details of the PIMC simulations can be found in ref 31. Briefly, the PIMC simulations are performed for a system of N = 1000 atoms located in a cubic box, with periodic boundary conditions. Each atom is represented by a ring-polymer with $n_b = 10$ beads (for h > 0; $n_b = 1$ for h = 0); additional PIMC simulations are included in the Supporting Information (SI) using different values of n_b . Simulations are performed at constant temperature and volume. In one MC step, we first attempt to move all of the 10000 beads. This is followed by MC moves where the ring-polymer centers of mass (centroids)

are attempted to move. The systems are equilibrated for 10⁶ MC steps and simulations are run for at least 10⁶ additional MC steps for data analysis. After equilibration, we save configurations of the system every 10000 MC steps and the corresponding inherent structures (local potential energy minimum) are obtained by using the conjugate gradient algorithm.³⁴ Hence, for each state point simulated, we calculate 100 IS.

We note that, in the case of classical liquids, the IS sampled by the system at a given T represent local minima where the system would end up under an extremely fast-cooling process. In the case of quantum liquids, this is no longer the case. This is because (i) during the potential energy minimization procedure at a given T, the spring constant remains unchanged. Instead, (ii) during a fast-cooling process, the spring constant associated with the quantum liquid/ring-polymer system decreases with decreasing temperature (see Section 3.1.1). In other words, processes (i) and (ii) are fundamentally different in the quantum case.

3. RESULTS

3.1. Extending the Potential Energy Landscape Formalism to Quantum Liquids. In this section, we present in detail the PEL formalism extended to quantum liquids. Specifically, in Section 3.1.1 we briefly review the path-integral formalism of statistical mechanics that allows one to map the canonical partition function of the quantum liquid to the canonical partition function of a classical ring-polymer system. The PEL formalism extended to the case of quantum liquids is discussed in Section 3.1.2, and the corresponding harmonic and Gaussian approximations are discussed in Sections 3.1.3 and 3.1.4.

3.1.1. Isomorphism between the Quantum Liquid and Classical Ring-Polymer Systems. The canonical partition function of a quantum liquid composed of N atoms is given by

$$Q(N, V, T) = Tr(\hat{\rho})$$

where ${\rm Tr}(\hat{\rho})$ is the trace of the density operator $\hat{\rho}=\exp(-\beta\hat{H})$ and

$$\hat{H} = \sum_{i=1}^{N} \frac{\hat{\mathbf{p}}_{i}^{2}}{2m_{i}} + U(\hat{\mathbf{r}}_{1}, \, \hat{\mathbf{r}}_{2}, \, ..., \, \hat{\mathbf{r}}_{N})$$
(2)

is the Hamiltonian operator of the system. In this expression, $(\hat{\mathbf{r}}_i, \hat{\mathbf{p}}_i)$ are the position and momentum operators associated with atom i = 1, 2, ..., N, and $\beta = 1/k_BT$; k_B is the Boltzmann's constant.

Using the path-integral formulation of statistical mechanics, one can show that the canonical partition function of the quantum liquid is identical to the canonical partition function of a *classical* system composed of N distinguishable ringpolymers of $n_b \rightarrow \infty$ distinguishable beads, and with peculiar interactions. Specifically, it can be shown that

$$Q(N, V, T) = \lim_{n_b \to \infty} \frac{1}{h^{3n_b N}} \int_{V} \left(\prod_{i=1}^{N} d\mathbf{r}_i^1 \cdots d\mathbf{r}_i^{n_b} \right)$$
$$\int_{-\infty}^{\infty} \left(\prod_{i=1}^{N} d\mathbf{p}_i^1 \cdots d\mathbf{p}_i^{n_b} \right) \exp(-\beta \mathcal{H}_{RP}(\mathbf{P}, \mathbf{R}))$$
(3)

where

$$\mathcal{H}_{RP}(\mathbf{P}, \mathbf{R}) = \sum_{i=1}^{N} \sum_{k=1}^{n_b} \frac{(\mathbf{p}_i^k)^2}{2m'_i} + \sum_{i=1}^{N} \sum_{k=1}^{n_b} \frac{1}{2} k_{sp} (\mathbf{r}_i^{k+1} - \mathbf{r}_i^k)^2 + \frac{1}{n_b} \sum_{k=1}^{n_b} U(\mathbf{r}_1^k, \mathbf{r}_2^k ..., \mathbf{r}_N^k)$$
(4)

is the Hamiltonian of the ring-polymer system and $k_{sp} = mn_b/(\hbar\beta)^2$ is the (temperature dependent) spring constant of the ring-polymers. In this expression, $(\mathbf{r}_i^k, \mathbf{p}_i^k)$ are the vector position and momentum of the kth bead of the ith ring-polymer $(i=1,2,...,N,k=1,2,...,n_b)$. In eq 4, the mass of the beads belonging to ring-polymer i is given by $m'_i = n_b m_i$; however, the specific value of m'_i plays no relevant role in the thermodynamic properties derived from Q(N,V,T). Note that in eq 4 and throughout this work, $\mathbf{r}_i^{n_b+1} = \mathbf{r}_i^1$ for $i \in \{1,2,...,N\}$, i.e., the polymers are ring-polymers.

It follows from eq 4 that the potential energy of the ringpolymer system is given by

$$\mathcal{U}_{RP}(\mathbf{R}) = \sum_{i=1}^{N} \sum_{k=1}^{n_b} \frac{1}{2} k_{sp} (\mathbf{r}_i^{k+1} - \mathbf{r}_i^k)^2 + \frac{1}{n_b} \sum_{k=1}^{n_b} U(\mathbf{r}_1^k, \mathbf{r}_2^k, ..., \mathbf{r}_N^k)$$
(5)

In this peculiar ring-polymer system, only beads with the same label k interact with each other. The set of all beads with the same label k is usually referred to as the replica k of the system, and the term $U(\mathbf{r}_1^k, \mathbf{r}_2^k, ..., \mathbf{r}_N^k)$ in eqs 3 and 5 is the total potential energy of replica k [the function U(...) is defined in eq 2]; beads belonging to different replicas do not interact with one another.

Strictly speaking, eq 3 provides the exact canonical partition function of the quantum liquid if $n_b \to \infty$. In computational studies, one chooses a sufficiently large value of n_b for which the properties of the system of interest converge; i.e., they no longer vary upon further increase in n_b . This implies that one can associate a well-defined configurational space with the quantum liquid (for a fixed value of n_b). In particular, the potential energy of the ring-polymer system given in eq 5 defines a PEL for the quantum liquid. The main difference between the PELs of a classical and a quantum system is that the PEL of the quantum liquid is T-dependent, since $k_{sp} \propto T^2$, while the PEL is T-independent for classical systems.

3.1.2. A PEL for the Quantum Liquid. Next, we apply the PEL formalism to the quantum liquid/ring-polymer system defined by eq 5. The presentation below follows closely the standard introduction to the PEL formalism for classical systems (see, e.g., refs 10, 18, and 20), but it takes into consideration the fact that the PEL for a quantum liquid is *T*-dependent (eq 5).

The main idea of the PEL formalism is to partition the PEL into basins. ¹⁰ Each basin of $\mathcal{U}_{RP}(\mathbf{R})$ is characterized by a local (potential energy) minimum, or inherent structure (IS), and the corresponding basin is defined as the set of points in $\mathcal{U}_{RP}(\mathbf{R})$ that converge to the given IS by steepest descent (i.e., upon potential energy minimization). With this partition of the PEL, eq 3 can be written as

$$Q(N, V, T) \approx \frac{1}{h^{3n_b N}} \sum_{basin \ I'} \int_{V_I} dr^{3n_b N} \int_{-\infty}^{\infty} dp^{3n_b N} e^{-\beta \mathcal{H}_{RP}}$$
(6)

where l' is a label that identifies the different basins of the PEL and $V_{l'}$ is the volume within the configurational space associated with basin l'. Moreover, one can group the basins of the PEL by the corresponding IS energy, e_{IS} , and replace $\sum_{basin \ l'} \rightarrow \sum_{e_{IS}} \sum_{basin \ l(e_{IS})}$. Here, $\sum_{e_{IS}}$ is a sum that runs over all values of the IS energies e_{IS} available in the PEL; the sum $\sum_{basin \ l(e_{IS})}$ runs over all basins l of the PEL with corresponding IS energy equal to e_{IS} . It follows that eq 6 can be written as

$$Q(N, V, T) = \frac{1}{h^{3n_b N}} \sum_{e_{IS}} \sum_{basin \ l(e_{IS})} \int_{V_I} dr^{3n_b N} \int_{-\infty}^{\infty} dp^{3n_b N} e^{-\beta \mathcal{H}_{RP}}$$
(7)

When the system is moving within the basin l of the PEL, its potential energy can be written as $\mathcal{U}_l(\mathbf{R}) = e_{lS} + \Delta \mathcal{U}_l(\mathbf{R})$, where $\Delta \mathcal{U}_l$ is the potential energy of the system relative to the basin minimum energy, e_{lS} . Using this expression, eq 7 can be written as

$$Q(N, V, T) = \sum_{e_{IS}} e^{-\beta e_{IS}} \sum_{basin \ l(e_{IS})} \left(\frac{1}{h^{3n_b N}} \int_{-\infty}^{\infty} e^{-\beta \sum_{i=1}^{N} \sum_{k=1}^{n_b} (\mathbf{p}_i^k)^2 / 2m'_i} d\mathbf{p}^{3n_b N} \right)$$

$$\int_{V_i} e^{-\beta \Delta U_i} d\mathbf{r}^{3n_b N}$$
(8)

The parentheses in eq 8 indicate the canonical partition function of basin l, $Q_l(N, V, T)$, when the reference value for the potential energy of the system is set to zero at the corresponding IS. Specifically,

$$Q_{l}(N, V, T) = \frac{1}{h^{3n_{b}N}} \int_{-\infty}^{\infty} e^{-\beta \sum_{i=1}^{N} \sum_{k=1}^{n_{b}} (\mathbf{P}_{i}^{k})^{2}/2m'_{i}} dp^{3n_{b}N}$$
$$\int_{V_{l}} e^{-\beta \Delta \mathcal{U}_{l}} dr^{3n_{b}N}$$
(9)

and hence,

$$Q(N, V, T) = \sum_{e_{IS}} e^{-\beta e_{IS}} \sum_{basin \ l(e_{IS})} Q_{l}(N, V, T)$$
(10)

Next, we introduce two important definitions that allow one to rewrite eq 10 in a more useful form. First, we introduce the configurational entropy,

$$S_{IS}(N, V, T; e_{IS}) \equiv k_{\rm B} \ln[\Omega_{IS}(N, V, T; e_{IS})]$$
 (11)

where $\Omega_{IS}(N, V, T; e_{IS})$ is the number of IS available in the PEL with energy e_{IS} (at constant (N, V, T)). Note that, contrary to the case of classical systems, Ω_{IS} and, hence, S_{IS} are now explicit functions of T. The definition of $S_{IS}(N, V, T; e_{IS})$ is evidently motivated by Boltzmann's definition of entropy. The second definition we introduce is the vibrational Helmholtz free energy of the system, $F_{vib}(N, V, T; e_{IS})$, in the imaginary situation where the system is only allowed to visit IS with energy e_{IS} ,

$$F_{vib}(N, V, T; e_{IS}) \equiv -k_{B}T \ln(\langle Q_{l}(N, V, T) \rangle_{e_{IS}})$$
(12)

Here, $\langle Q_l(N, V, T) \rangle_{e_{lS}}$ is the average partition function over all basins l with energy e_{lS} , i.e.,

$$\langle Q_{I}(e_{IS})(N, V, T) \rangle$$

$$\equiv \frac{1}{\Omega_{IS}(N, V, T; e_{IS})} \sum_{basin \ I(e_{IS})} Q_{I}(N, V, T)$$
(13)

Equation 12 provides the single contribution to the Helmholtz free energy that arises from the microstates belonging to the

basins with IS energy e_{IS} . By using eqs 11, 12, and 13 in eq 10, one obtains the following compact expression for the canonical partition function of the system 10,18,20

$$Q(N, V, T) = \sum_{e_{IS}} e^{-\beta(e_{IS} - TS_{IS}(N, V, T; e_{IS}) + F_{vilb}(N, V, T; e_{IS}))}$$
(14)

3.1.2.1. The Only Approximation of the PEL Formalism. While, within the PEL formalism, eq 14 is exact (it involves no assumption or approximation), it is of limited practical use. Equation 14 can be reduced to a more practical form by noticing that the argument of $\exp(...)$ is proportional to $N.^{10}$ Hence, in the thermodynamic limit, only the term that maximizes the sum in eq 14 should be dominant. Indeed, in the PEL formalism, one uses a saddle-point approximation in eq $14:^{10,18,20}$

$$Q(N, V, T) \approx e^{-\beta(E_{IS} - TS_{IS}(N, V, T; E_{IS}) + F_{vib}(N, V, T; E_{IS}))}$$
(15)

where $E_{IS}(N, V, T)$ is the IS energy that maximizes the argument in the sum of eq 14. Specifically, $E_{IS}(N, V, T)$ is the solution of

$$1 - T \left(\frac{\partial S_{IS}(N, V, T; e_{IS})}{\partial e_{IS}} \right)_{N,V,T} + \left(\frac{\partial F_{vib}(N, V, T; e_{IS})}{\partial e_{IS}} \right)_{N,V,T} = 0$$
at $e_{IS} = E_{IS}$ (16)

Equation 15 also follows by assuming that, at the working conditions, the system can only sample a very narrow distribution of e_{IS} -values, with $e_{IS} \approx E_{IS}$. This is indeed found in computer simulations of finite-size atomistic and molecular classical systems (see, e.g., ref 37). In computational studies, E_{IS} is identified with the average value of the IS energies e_{IS} sampled by the liquid in equilibrium (at a given (N, V, T)). We note, however, that this picture may break down across first-order phase transitions where the distributions of IS-energies may become bimodal (see, e.g., refs 38, 39, and 40).

- 3.1.3. The Gaussian and Harmonic Approximations for the PEL. There are two important approximations that are commonly used to study the properties of classical liquids and glasses using the PEL formalism: (i) The Gaussian approximation of the PEL, which assumes that $\Omega_{IS}(e_{IS})$ is a Gaussian distribution; and (ii) the harmonic approximation (HA), which assumes that the basins of the PEL have a parabolic (quadratic) shape about the IS [in (3N+1)-dimensional space]. 10,18,20,41 Approximation (i) allows one to calculate analytically $S_{IS}(N, V, T; E_{IS})$; approximation (ii) allows one to calculate analytically $F_{vib}(N, V, T)$. Together, approximations (i) and (ii) allow one to write a closed expression for Q(N, V, T) (see eq 15) from which all the thermodynamic properties follow.
- (i) In the Gaussian approximation of the PEL, one assumes that the distribution of IS energies in the PEL is given by

$$\Omega_{IS}(N, V, T; e_{IS}) = \frac{1}{\sqrt{2\pi}\sigma} e^{\alpha N} e^{-(e_{IS} - E_0)^2/2\sigma^2}$$
(17)

where, for classical systems, α , E_0 , and σ depend only on V. In the case of quantum liquids, however, one may expect that $\alpha = \alpha(V, T)$, $E_0 = E_0(V, T)$, and $\sigma = \sigma(V, T)$ since the PEL varies with T. Equation 17 implies that, in equilibrium (i.e., $e_{IS} \rightarrow E_{IS}$), the configurational entropy is given by (see eq 11)⁴¹

$$S_{IS}(N, V, T; E_{IS}) \approx k_{\rm B} \left[\alpha N - \frac{(E_{IS} - E_0)^2}{2\sigma^2} \right]$$
 (18)

(ii) In the HA of the PEL, one assumes that the basins of the PEL, about the corresponding IS, are quadratic functions. ¹⁰ This allows one to calculate the Helmholtz free energy of the independent basins of the PEL (eq 9). As shown in the SI, in the HA of the PEL,

$$F_{vib}(N, V, T) \approx 3Nn_b k_B T \ln(\beta \hbar \omega_0) + k_B T S(N, V, T; E_{IS})$$
(19)

where

$$S(N, V, T; E_{IS}) \equiv \left\langle \ln \left(\prod_{j=1}^{3n_b N} (\omega_j/\omega_0) \right) \right\rangle_{E_{IS}}$$
 (20)

is the so-called basin-shape function 20 (in equilibrium, $e_{IS} \rightarrow E_{IS}$). In this expression, the $3n_bN$ values $\{\omega_j^2\}$ are the eigenvalues of the Hessian matrix of the ring-polymer system at the IS with energy $e_{IS} = E_{IS}$, and $\langle ... \rangle_{E_{IS}}$ indicates an average over all basins of the PEL with energy $e_{IS} = E_{IS}$. While for classical systems $\omega_j = \omega_j(N, V; e_{IS})$, for quantum liquids, $\omega_j = \omega_j(N, V, T; e_{IS})$. The constant ω_0 is an arbitrary quantity that makes the argument of $\ln(...)$ in eqs 19 and 20 unitless. 20 $S(N, V, T; e_{IS})$ is a very important property of the PEL that quantifies the average local curvature of the basins with IS energy equal to e_{IS} ; it is the only term in eq 19 that makes F_{vib} dependent on the PEL of the system.

3.1.3.1. Energy of the Quantum Liquid. Using the Gaussian and harmonic approximations of the PEL, one can obtain all of the thermodynamic properties of the quantum liquid using eq 15. In particular, the energy of the quantum liquid is given by $E(N, V, T) = -\left(\frac{\partial \ln Q(N, V, T)}{\partial \beta}\right)_{N, V}$ which, using eq 15, can be

written as

$$E(N, V, T) = E_{IS} + \left[\beta \left(\frac{\partial E_{IS}}{\partial \beta} \right)_{N,V} - \frac{1}{k_B} \left(\frac{\partial S_{IS}(N, V, T; E_{IS})}{\partial \beta} \right)_{N,V} + \left(\frac{\partial (\beta F_{vib}(N, V, T; E_{IS}))}{\partial \beta} \right)_{N,V} \right]$$

$$(21)$$

The second term in the expression above is the so-called vibrational energy,

$$E_{vib} \equiv E - E_{IS} = \left[\beta \left(\frac{\partial E_{IS}}{\partial \beta} \right)_{N,V} - \frac{1}{k_B} \left(\frac{\partial S_{IS}(N, V, T; E_{IS})}{\partial \beta} \right)_{N,V} + \left(\frac{\partial (\beta F_{vib}(N, V, T; E_{IS}))}{\partial \beta} \right)_{N,V} \right]$$

$$(22)$$

and represents the energy of the ring-polymer system due to the exploration of the PEL basins about the corresponding IS. Using eqs 18 and 19 in eq 16, one obtains

$$E_{IS}(N, V, T) = E_0 - \sigma^2(\beta + b)$$
 (23)

where $b \equiv \left(\frac{\partial S(N,V,T,E_{\rm IS})}{\partial E_{\rm IS}}\right)_{N,V,T}$. Interestingly, in classical atomic and molecular systems, it is usually found that b=b(N,V), i.e., $S(N,V;E_{\rm IS})=a(N,V)+b(N,V)E_{\rm IS}$.

Similarly, using eqs 18, 19, and 23 in eq 22, it can be shown that

$$E_{vib}(N, V, T) = 3Nn_b k_B T + \left[\left(\frac{\partial S}{\partial \beta} \right)_{N,V,E_{IS}} - N \left(\frac{\partial \alpha}{\partial \beta} \right)_{V} + (\beta + b) \left(\frac{\partial E_0}{\partial \beta} \right)_{V} - \frac{(\beta + b)^2}{2} \left(\frac{\partial \sigma^2}{\partial \beta} \right)_{V} \right]$$
(24)

The square brackets in this expression are unique to the quantum liquid. This is because for classical systems, the PEL is T-independent and, hence, so are S, α , E_0 , and σ . Indeed, it has been shown that, for a classical system composed of N atoms, $E_{vib} = 3Nk_BT$, $E_{vib} = 3Nk_BT$, in agreement with eq 24.

3.1.4. IS with Collapsed Ring-Polymers. In a previous study²² based on PIMC simulations of the QFJ liquid, we noticed that the ring-polymers collapsed when the system was found at an IS. The PIMC simulations of ref 22 were performed at v=2.2, $T \leq 5.0$, and $h=h_1$, h_2 , h_3 , and h_4 , but we find that the collapsing of the ring-polymers onto a single point, when the system is at an IS, seems to be a rather general result. As shown in the SI, additional PIMC simulations of the QFJ liquids over a wide range of volumes v=1.0-6.0 and h show that, even at low temperatures, the ring-polymers collapse at the IS; the range of v considered expand over the whole liquid state, from the vapor spinodal to the ultradense liquid state.⁴⁰

The collapse of the ring-polymers at the IS of the RP-PEL provides an important simplification of the PEL formalism when applied to quantum liquids; specifically, it makes the calculation of the shape function straightforward. This is because, when the ring-polymers are collapsed, the IS sampled by the ring-polymer system in the RP-PEL are also IS of the associated N-atoms system (in the N-particle "classical" PEL, CL-PEL).²² Specifically, under these conditions, the IS of the RP-PEL is defined by $\mathbf{R}_1 = \mathbf{R}_2 = ... = \mathbf{R}_{n_b} \equiv \mathbf{R}_{IS}$ (where we denote $\mathbf{R}_k = (\mathbf{r}_1^k, ..., \mathbf{r}_N^k)$, i.e., all replicas are identical, and the N-atoms classical configuration defined by R_{IS} defines an IS of the CL-PEL (see ref 22). As shown in the Appendix, this implies that the normal modes of (i) the ring-polymer system at the IS of the RP-PEL can be obtained from (ii) the normal modes of the associated N-atoms system at the corresponding IS of the CL-PEL.

In the Appendix, we show that the normal modes frequencies of the ring-polymer system at the IS of the RP-PEL, $\{\omega_{i,i}\}$, are given by

$$\omega_{i,j}^{2} = \frac{\omega_{i,0}^{2}}{n_{b}} - 2k_{sp} \left[\cos \left(\frac{2\pi}{n_{b}} j \right) - 1 \right]$$
(25)

where $\{\omega_{i,0}\}$ are the normal modes frequencies of the associated N-atoms system at the IS of the CL-PEL defined by \mathbf{R}_{IS} . In eq 25, i=1,2,...,3N and $j=1,2,...,n_b$ and, hence, a given frequency $\omega_{i,0}$ of the N-atoms system gives rise to a set of n_b frequencies of the ring-polymer system, $\{\omega_{i,j}\}_{j=1,2,...,n_b}$. Equation 25 is similar to eq 2.38 of ref 42 obtained independently, in the application of the instanton method to transition state theory.

Note that $\omega_{i,j=n_b} = \frac{\omega_{i,0}}{\sqrt{n_b}}$ and, hence, the vibrational frequencies of the ring-polymer system for $j=n_b$ are equal to the vibrational frequencies of the associate N-atoms system, rescaled by the factor $1/\sqrt{n_b}$. Moreover, as shown in the

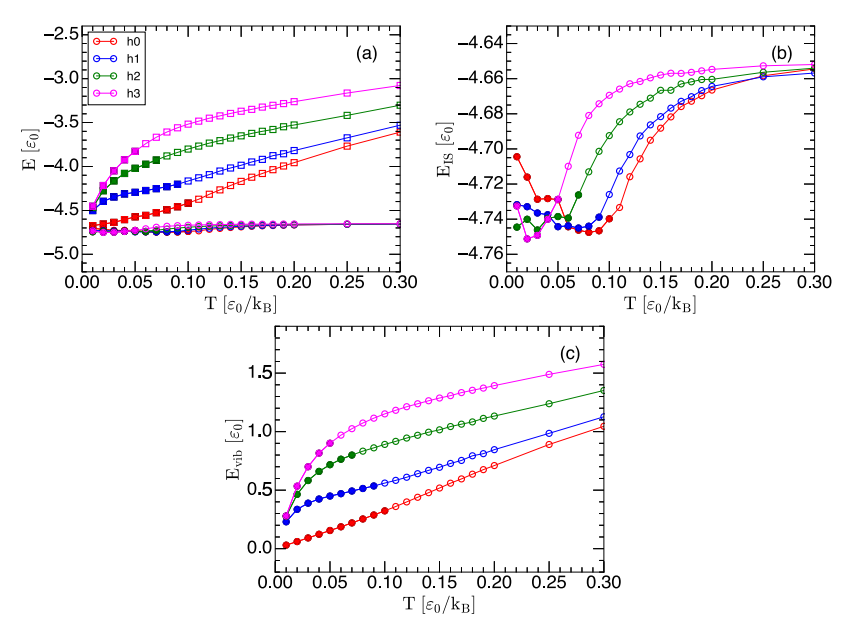


Figure 2. (a) Total energy of the quantum FJ liquids with different values of the Planck's constant h and at v = 2.2 (squares). Also included are the corresponding IS energies (circles). (b) Magnification of the IS energies sampled by the quantum liquids/ring-polymer systems included in (a). As h increases, and the liquid becomes more quantum, $E_{IS}(T)$ shifts toward lower temperatures. (c) Vibrational energy per particle obtained from (a) and (b); $E_{vib}(T) = E(T) - E_{IS}(T)$. All energies are given per atom (i.e., divided by the number of atoms N). Empty and solid symbols correspond to equilibrium and out-of-equilibrium states, respectively.

Appendix, in these normal modes, the ring-polymers remain collapsed at all times and oscillate in the same manner as the classical particles do when the vibrational frequency is ω_{i0} .

3.2. Computer Simulations of a Quantum Liquid: Testing the PEL Formalism. In this section, we compare the predictions for $E_{IS}(N, V, T)$ and $E_{vib}(N, V, T)$ from the Gaussian and harmonic approximations of the PEL (eqs 23 and 24) with results from PIMC simulations of the FJ liquid. In particular, we find that the PEL properties of (i) the ringpolymer/quantum liquid (RP-PEL) and (ii) the associated N-atoms classical system (CL-PEL) behave qualitatively differently. For simplicity, we will assume that α , E_0 , and σ have a very weak or null T-dependence so eq 24 can be approximated by

$$E_{vib}(N, V, T) = 3Nn_b k_B T + \left(\frac{\partial S}{\partial \beta}\right)_{N, V, E_{IS}}$$
 (26)

Briefly, we show that our PIMC simulations for the QFJ model at $\nu = 2.2$ are in very good agreement with eq 23 at low temperature and with eq 26 at very low temperatures. Importantly, we also validated eq 25.

In order to identify the relevant T-interval for the QFJ liquids considered, we include in Figure 2 the (a) total energy E(T), (b) IS energy $E_{IS}(T)$, and (c) vibrational energy $E_{vib}(T)$ of the QFJ liquids with $h=h_0$, h_1 , h_2 , and h_3 from PIMC simulations ($\nu=2.2$). Briefly, the qualitative behavior of $E_{IS}(T)$ is common to all QFJ liquids studied, independently of h, i.e., of the quantum character of the liquid. At high temperatures, approximately T>0.20-0.25, $E_{IS}(T)$ is approximately constant, while at lower temperatures, $E_{IS}(T)$ decreases rapidly until crystallization intervenes or the liquid is no longer in equilibrium (empty and solid symbols indicate, respectively, the temperatures at which the liquid reaches/does not reach equilibrium within the total number of PIMC simulation steps). The PEL approach is of practical use in the T range

where $E_{IS}(T)$ is temperature dependent.⁴¹ Accordingly, based on Figure 2, one may want to focus on the temperatures T < 0.25-0.30. Alternatively, one may want to focus on the T-range of the equilibrium liquid where the values of E_{IS} are not negligible, for example, at temperatures at which the total change in the IS energy $\Delta E_{IS} = E_{IS}(T) - E_{IS}(T=0) > 10\%$ $E_{vib}(T)$. Since $\Delta E_{IS} < 0.1$, this implies that the relevant temperatures are those for which $E_{vib}(T) < 1.0$. In this case, the temperatures of interest are approximately T < 0.06 $(h = h_3)$, T < 0.13 $(h = h_2)$, T < 0.25 $(h = h_1)$, and T < 0.30 $(h = h_0)$.

3.2.1. Harmonic Approximation of the PEL. In order to test eq 26, we first confirm that eq 25 is consistent with our PIMC simulations. Figure 3 shows the probability distribution of the normal modes vibrational frequencies, $P(\omega)$, for the ring-polymer system with $h=h_3$, when the system is at the IS of the PEL [the vibrational frequencies are the square-root of the eigenvalues of the Hessian matrix associated with the ring-polymer system (at the IS)]. At very high temperatures, e.g., T=0.50, $P(\omega)$ shows a wide peak at $\omega<8$ and a few sharp peaks at higher frequencies. The wide peak at $\omega<8$ corresponds to the frequencies given in eq 25 with $j=n_b$, i.e., $\omega_{i,j=n_b}=\frac{\omega_{i,0}}{\sqrt{n_b}}$.

Hence, these frequencies correspond to the normal-mode frequencies of the corresponding classical liquid. Indeed, we find that this wide maximum overlaps with the distribution $P_0(\omega)$ obtained for the case $h=h_0$, after rescaling the frequencies by $1/\sqrt{n_b}$. The sharp peaks at $\omega>8$ are due to the presence of the springs in the ring-polymer system (second term in eq 25 for $j < n_b$). Since $k_{sp} \propto T^2$, the location of the sharp peaks shown in Figure 3a shift toward lower temperatures upon cooling [Figure 3b-h]. At approximately T < 0.15, the low- and high-frequency peaks fully overlap and there is no trace of $P_0(\omega)$ in the corresponding $P(\omega)$.

The distributions $P(\omega)$ obtained from the PIMC simulations are also compared with the theoretical prediction (eq 25) in Figure 3. The agreement between the PIMC simulations and

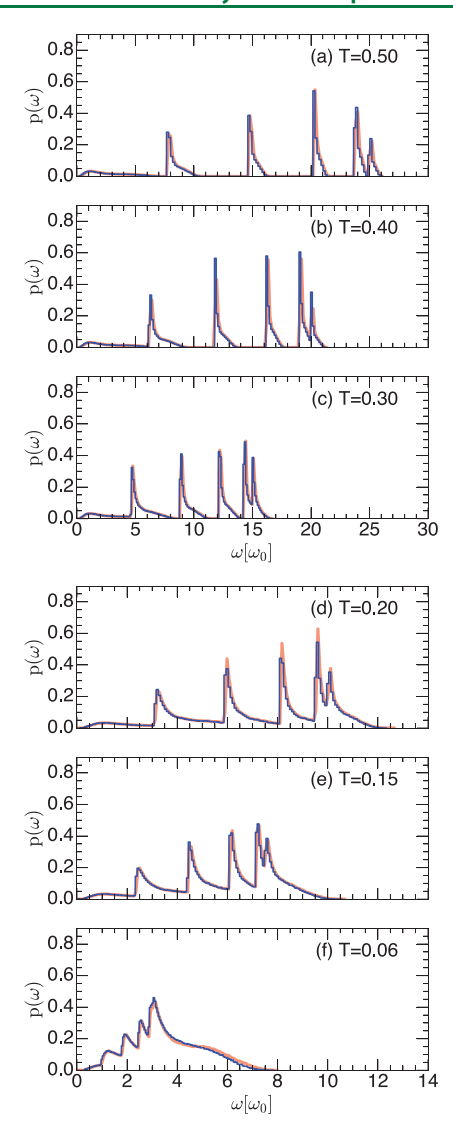


Figure 3. Inherent structure normal-mode frequencies distribution, $P(\omega)$, of the ring-polymer system associated with the QFJ liquid. Results are from PIMC simulations using a Planck's constant $h=h_3$. $P(\omega)$ shifts to lower frequencies with decreasing temperatures. Red lines correspond to the frequencies obtained numerically, by calculating the eigenvalues of the Hessian matrix of the ring-polymer system; blue lines are the frequencies given by eq 25.

the theory is remarkable; a similar agreement is found at $h = h_1$ and h_2 over a wide range of temperatures ($\nu = 2.2$); for example, see Figure 4 and the SI. It follows from eq 20 that a similar agreement, between PIMC simulations and theory, holds for the case of S as well; see Figure 5.

The T-dependence of the shape function is remarkably different for the classical $(h=h_0)$ and quantum FJ liquids $(h=h_1,h_2,h_3)$. As shown in the inset of Figure 5, for the classical FJ liquid, S(T) is constant at high temperatures (T>0.20) and increases very slightly at low temperatures, before the system is no longer in the equilibrium liquid state (T<0.09). Instead, for the quantum liquids, S(T) decreases monotonically upon cooling. This implies that while for classical liquids the shape of the basins about the corresponding IS remains constant or becomes slightly thinner (larger curvature) upon cooling, for the quantum liquids/ring polymer systems the basins become wider (smaller curvature) with decreasing temperature.

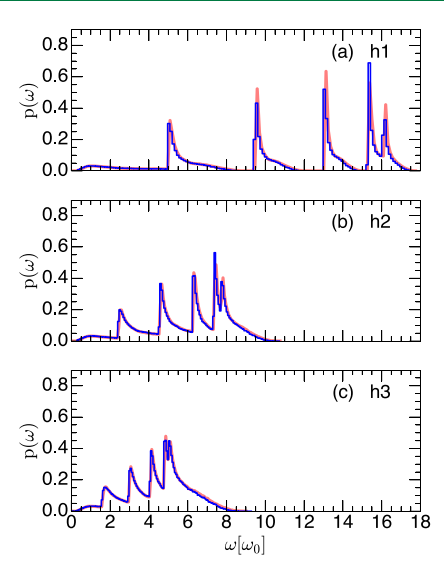


Figure 4. Distribution of IS normal-mode frequencies $P(\omega)$ of the ring-polymer systems associated with the QFJ liquids with Planck's constant (a) $h = h_1$, (b) $h = h_2$, and (c) $h = h_3$. The temperature is T = 0.10 in all cases. Red lines correspond to the frequencies obtained numerically, by calculating the eigenvalues of the Hessian matrix of the ring-polymer systems; blue lines are the frequencies given by eq 25.

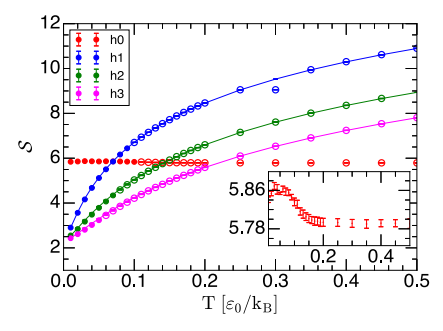


Figure 5. Shape function (per particle) divided by the number of beads per ring-polymer, n_b , as a function of temperature from PIMC simulations at $\nu=2.2$ (circles). Results are for the QFJ liquids with Planck's constant $h=h_1$, h_2 , h_3 . Lines are the theoretical results based on eqs 20 and 25. Also included is the shape function (per particle) for the classical FJ liquid ($h=h_0=0$, red circles) (also shown in the inset). Empty and solid symbols correspond, respectively, to equilibrium and out-of-equilibrium states. For the quantum liquids/ring-polymer system (h>0), the shape function decreases monotonically with decreasing temperatures, i.e., the RP-PEL basins become wider upon cooling, Instead, in the classical case (inset), the shape function increases slightly with decreasing temperatures.

Next, we compare the T-dependence of E_{vib} obtained from PIMC simulations of the QFJ liquids with the corresponding prediction of the PEL formalism given by eq 26, based on the harmonic and Gaussian approximations. At first sight, this may seem straightforward to do since S(T) is given in Figure 5. However, the second term in eq 26 is not the slope resulting from Figure 5 since the partial derivative in eq 26 must be calculated at a constant E_{IS} . Therefore, to calculate $\left(\frac{\partial S}{\partial \beta}\right)_{N,V,E_{IS}}$,

we take advantage of eqs 20 and 25, and calculate $\mathcal{S}(T, e_{IS})$ as explained below.

As discussed in Section 3.1.4, we only need to consider the IS of the RP-PEL for which all of the ring-polymers are

collapsed. Under these conditions, an IS of the RP-PEL is also an IS of the CL-PEL 22 It can be shown that the opposite is also true, i.e., an IS of the CL-PEL is also an IS of the RP-PEL with collapsed ring-polymers.⁴⁶ It follows that there is a one-toone relationship between the IS of the CL-PEL and the IS of the RP-PEL with collapsed ring-polymers. Therefore, to calculate $S(T, e_{IS})$, we first obtain the IS from the classical N-atom system, using classical MC simulations ($n_b = 1$). Each of these IS of the CL-PEL has a well-defined energy e_{IS} and curvatures $\{\omega_{i,0}\}\ (i=1,\ 2,\ ...,\ 3N)$. We then obtain the corresponding curvatures $\{\omega_{i,j}\}$ $(i = 1, 2, ..., 3N \text{ and } j = 1, 2, ..., n_b)$ of the RP-PEL using eq 25. The shape function of the PR-PEL for the given IS with energy e_{IS} is then calculated by using eq 20. Summarizing, $S(T, e_{IS})$ is obtained from IS sampled by the classical liquid in MC simulations, and using the analytical expression in eq 25 to get the corresponding curvatures at any temperature T. Figure 6 shows the so obtained $S(T, e_{IS})$ as a

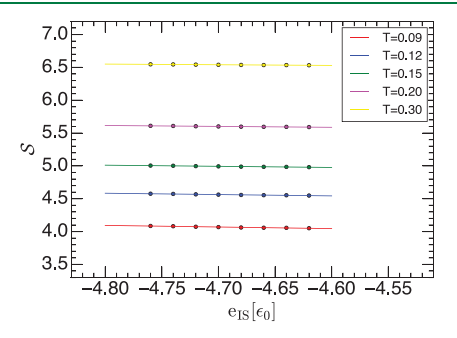


Figure 6. Shape function of the ring-polymer system/QFJ liquid as a function of e_{IS} , at selected temperatures and for the case $h = h_3$ (similar results hold for $h = h_0$, h_1 , h_2). Straight lines are guides to the eye.

function of e_{IS} , for selected values of T. We find that, for a given T ($\nu = 2.2$ and N = 1000),

$$S(T, e_{IS}) \approx a(T) + b(T)e_{IS} \tag{27}$$

where the coefficients a(T) and b(T) are shown in Figure 7. Figure 8 shows $E_{vib}(T)$ obtained from the PIMC simulations at $h = h_1$, h_2 , and h_3 [solid/empty symbols; from Figure 2c] together with the prediction from eq 26 (lines). The agreement between PIMC simulations and the PEL approach is very good at low temperatures, at approximately $T \le 0.10$ -0.12 for $h = h_0$, h_1 , and $T \le 0.05$ at $h = h_2$, h_3 . We note that at the lowest temperatures (solid circles) the system is in the outof-equilibrium liquid state or in the glassy state (where the system is trapped in a basin of the RP-PEL). The deviations between PIMC simulations and the PEL predictions at higher temperatures (empty symbols) can be explained in terms of anharmonicities of the basins about the IS.²⁰ Indeed, even for the classical FJ liquid at T > 0.11, the behavior of $E_{vib}(T)$ deviates from the expected behavior based on the HA of the PEL, $E_{vib}(T) \approx 3Nk_BT$. Importantly, in the SI, we also perform PIMC simulations where the QFJ liquids are initially trapped at an IS, and then increase the temperature from T=0(heating runs). It is shown that eq 26 holds at low temperatures, while the system remains in the starting IS. Summarizing, our results strongly indicate that the HA approximation holds for the QFJ at very low temperatures, but anharmonicities of the RP-PEL basins are important at the low and intermediate temperatures at which the QFJ liquids

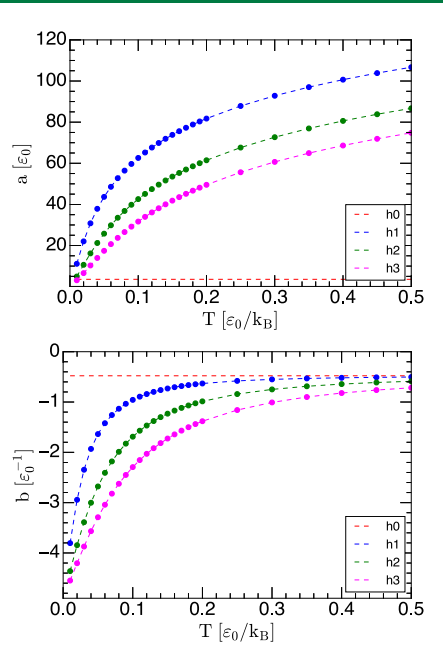


Figure 7. Parameters a(T) and b(T) resulting from Figure 6 and using eq 27.

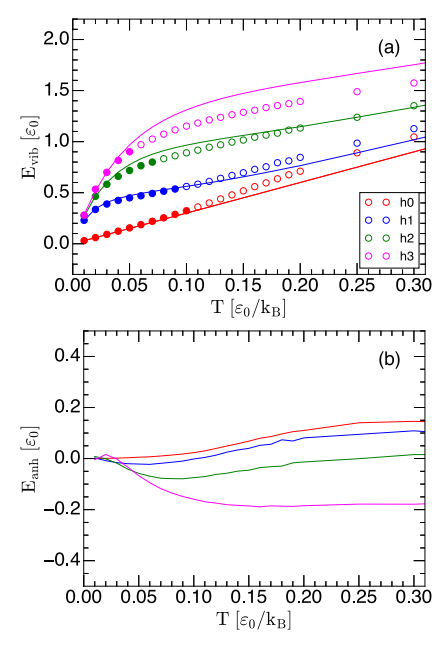


Figure 8. (a) Vibrational energy $E_{vib}(T)$ of the classical/quantum FJ liquids with Planck's constants $h=h_0$, h_1 , h_2 , h_3 [circles, taken from Figure 2c] together with the corresponding prediction from the PEL formalism using the harmonic and Gaussian approximations [lines, eq 26]. (b) Anharmonic contributions to $E_{vib}(T)$ calculated from (a). Anarmonicities are present at low temperatures, approximately T > 0.05-0.13, depending on h.

reach equilibrium. In this regard, we stress that the behavior of $E_{vib}(T)$ shown in Figure 8 for the quantum liquids (h > 0) is highly nontrivial, and very different from the corresponding behavior of the classical liquid (h = 0). Yet, eq 26 captures the differences between the cases h = 0 and h > 0.

3.2.2. Gaussian Approximation. In ref 22, we showed that, at low temperatures, the values of $E_{IS}(T)$ of the classical/quantum FJ liquids with $h = h_0$, h_1 , h_2 , h_3 were consistent with the Gaussian approximation of the PEL. In particular, it was

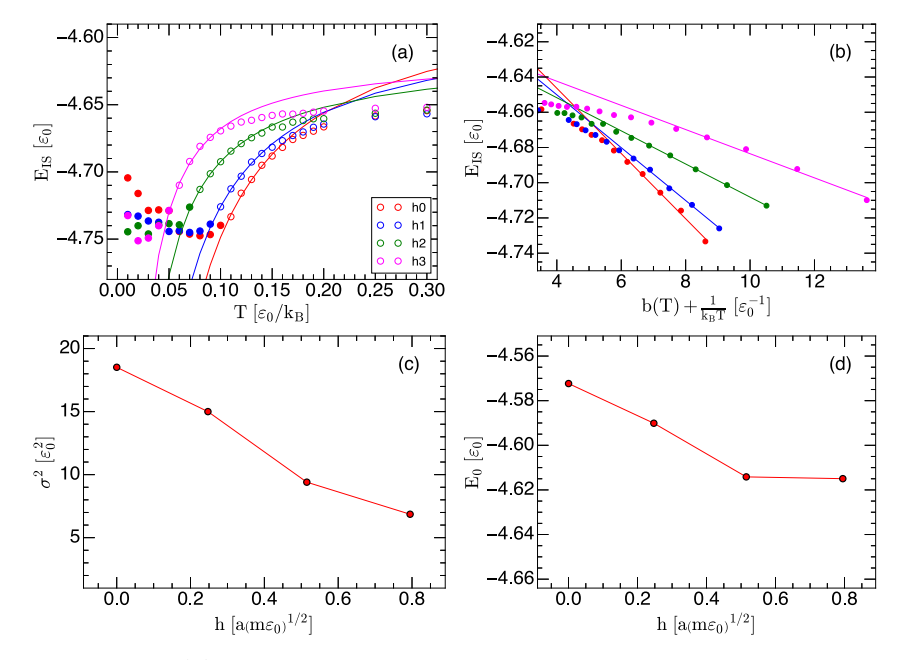


Figure 9. (a) Inherent structure energy $E_{IS}(T)$ of the classical/quantum FJ liquids with different Planck's constants h. Circles are results from the PIMC simulations [taken from Figure 2c]; lines are the predictions using the harmonic and Gaussian approximations of the PEL [eq 23 (lines)]. (b) $E_{IS}(T)$ [from (a)] as a function of $b(T) + \beta$ restricted to the T-interval where the Gaussian approximation of the PEL agrees with the results from the PIMC simulations. (c, d) Fitting parameters $\sigma^2(h)$ and $E_0(h)$ obtained from (b) using eq 23.

ı

found that, for all values of h considered, $E_{IS}(T) = E_0 - \sigma^2/(k_BT)$. However, this equation, and the results from ref 22, are based on the implicit assumption that b(N, V, T) = 0 (see the *definitions* introduced in eqs 23 and 24 of the SI in ref 22) which implies that the shapes of the basins of the PEL are independent of E_{IS} . In this section, we consider the general case where the quantity b is not necessarily equal to zero, and show that $E_{IS}(T)$ obeys eq 23 at low temperatures.

As shown in Figure 9a, the Gaussian and harmonic approximations of the PEL work remarkably well at intermediate temperatures. For example, for $h = h_3$, the PIMC simulation results for the equilibrium liquid (empty circles) overlap with the Gaussian and harmonic approximation predictions, eq 23 (lines), for $T \sim 0.05-0.12$. The Gaussian approximation does not hold at low temperatures because the quantum liquids become trapped in an out-ofequilibrium glass state; this is common in classical liquids.⁴⁸ For $h = h_3$, this happens at approximated T < 0.05 (solid symbols), i.e., at the same temperature at which the PIMC data (symbols) no longer overlap the predictions based on the Gaussian and harmonic approximation (lines). Deviations between the PIMC simulations results and eq 23 at high temperatures [in Figure 9a] or equivalently, at low $b(T) + \beta$ [in Figure 9b] are also expected and have been observed in many computational studies of classical liquids.⁴⁷ The Gaussian approximation is expected to hold only below the so-called onset temperature, 48 below which the relaxation of the liquid is no longer exponential, and $E_{IS}(T)$ starts to deviate from its plateau value at high temperatures (e.g., the onset temperature for $h = h_3$ is $T \sim 0.15$; see Figure 9a).

The fitting parameters $\sigma^2(h)$ and $E_0(h)$ defined in eq 23 are given in Figure 9c,d. Interestingly, both $\sigma^2(h)$ and $E_0(h)$ decrease with increasing h. This suggests that, as the liquid becomes more quantum, the distribution of IS energies available in the RP-PEL, $\Omega_{IS}(e_{IS}, T)$, (i) shifts slightly toward lower values of e_{IS} and (ii) becomes thinner (see also ref 22).

4. SUMMARY AND DISCUSSION

In this work, (i) we extend the PEL formalism to the case of quantum liquids and (ii) test the corresponding theoretical predictions with PIMC simulations of a monatomic model liquid (FJ model).

(i) Our presentation of the PEL formalism for quantum liquids is self-contained and is discussed in Section 3.1. Taking advantage of the isomorphism between quantum liquids and classical ring-polymer systems, in Section 3.1.1, we identify a PEL (RP-PEL) that can be associated univocally with the quantum liquid of interest (for a fixed number of beads, n_b). The PEL formalism is also revisited in Section 3.1.2 using the RP-PEL, stressing the differences between classical and quantum liquids. The main difference between these cases is that, for quantum liquids, the PEL is temperature-dependent, while, for classical liquids, it is not.

From a practical point of view, the PEL is important because, under a few physical assumptions, it provides a closed analytical form for the partition function of the system of interest (from which all of the thermodynamic properties of the system can be obtained). The most common assumptions that allow one to do so are the (a) Gaussian and (b) harmonic approximations. Accordingly, in Section 3.1.3, we also extend approximations (a) and (b) to the case of quantum liquids. It is shown that (a) and (b) lead to an expression for $E_{IS}(N, V, T)$ that is formally identical for quantum/classical liquids (eq 23). Instead, the expression for $E_{vib}(N, V, T)$ differs for quantum/classical liquids in a nontrivial manner (eq 24).

In ref 22, it was found that the ring-polymers of the FJ liquids collapse when the system is at an IS of the RP-PEL. The results from ref 22 are limited to v = 2.2. In this work, we perform additional simulations over a wide range of temperatures and volumes and confirm that, in all cases studied, the ring-polymers of the FJ liquids collapse at the IS of the RP-PEL. Accordingly, in Section 3.1, we also discuss the PEL formalism for the case where the ring-polymers are collapsed

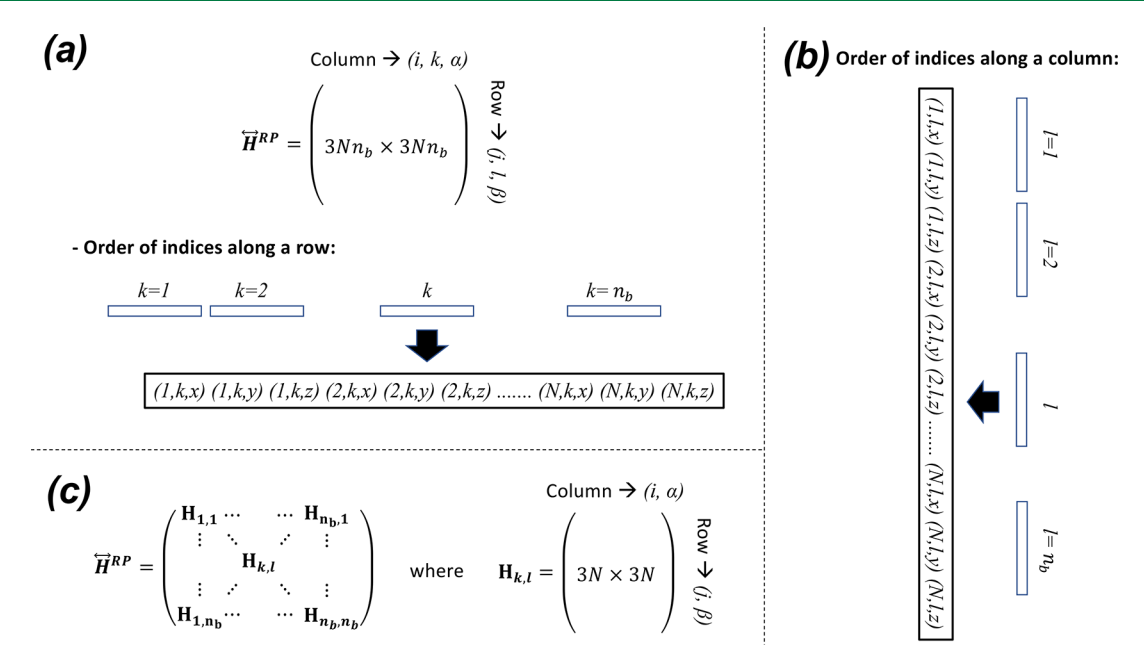


Figure 10. (a) Schematic diagram showing how the elements of the Hessian matrix, $[\mathbf{H}^{RP}]_{i,k,\alpha}^{l,l,k}$ are ordered within a given row with variable indices (i, k, α) . Along a row, all coordinates with the same value of k (replica number) are grouped together $(k = 1, 2, ..., n_b)$ increasing from left to right). Within the sequence of Hessian elements corresponding to replica k, the Hessian matrix elements are grouped depending on the ring-polymer number i = 1, 2, ..., N and component $\alpha = x, y, z$, as indicated. (b) A similar ordering of the Hessian matrix elements is used for any given column with variable indices (j, l, β) [j and l indicate, respectively, the ring-polymer and replica number; $\beta = x, y, z$. (c) The resulting Hessian matrix is a $(3n_bN \times 3n_bN)$ -square matrix composed of $(n_b \times n_b)$ blocks $H_{k,l}$ with $k = 1, 2, ..., n_b$ increasing from left to right, and $l = 1, 2, ..., n_b$ increasing from top to bottom. The blocks $H_{k,l}$ are $(3N \times 3N)$ -submatrices; see text.

when the system is at the IS of the RP-PEL. It is shown that when this is the case, the PEL formalism simplifies in a profound manner. Specifically, within the harmonic approximation, the eigenvalues and eigenvectors of the Hessian of the ring-polymer system can be calculated analytically from the eigenvalues/eigenvectors of the Hessian of the *classical N*-atoms systems (with the same potential energy as for the quantum liquid; see Appendix and Section 3.1.4).

(ii) In the second part of this work, we perform PIMC simulations of a family of quantum FJ liquids and test the predictions of the PEL formalism obtained in (i). Specifically, we find that the PIMC simulations are consistent with the PEL of the QFJ liquids being Gaussian (eq 23) at low temperatures and that the nontrivial behavior of the vibrational energy of the liquids is consistent with the harmonic approximation of the PEL (eq 26). In addition, we show that, as predicted in (i), the vibrational frequencies of the ring-polymer/quantum liquid can be obtained from the vibrational frequencies of the classical FJ liquid (eq 25).

Overall, our results indicate that the PEL formalism may indeed be applied to study low-temperature liquids and glasses that obey quantum mechanics. This allows for a common understanding of classical and quantum liquids in terms of the topography of the PEL. ^{10,20} It also allows for the inclusion of nuclear quantum effects in the PEL formalism to study atomic and molecular liquids/glasses. In the future, it would be important to test the present results for the case of atomic glass former systems, such as Lennard-Jones binary mixtures, as well as molecular systems, such as water.

APPENDIX: NORMAL MODES OF THE RING-POLYMER SYSTEM AT THE INHERENT STRUCTURES

In this Appendix, we calculate the eigenvalues and eigenvectors of the Hessian matrix associated with a classical system composed of N identical ring-polymers, each ring-polymer being composed of n_b beads. Motivated by the findings in the main manuscript, we limit ourselves to the case where (i) the system is trapped in an inherent structure (IS) of its potential energy landscape (RP-PEL), with (ii) every ring-polymer being collapsed onto a single point.

Let $\mathbf{r}_i^k \in \mathbb{R}^3$ denote the vector position of bead $k \in \{1, 2, ..., n_b\}$ that belongs to ring-polymer $i \in \{1, 2, ..., N\}$; $r_{i,\alpha}^k$ is the component of vector \mathbf{r}_i^k along the direction $\alpha \in \{x, y, z\}$. It follows that the configuration of the ring-polymer system is given by the vector $\mathbf{R} = (\mathbf{R}_1, \mathbf{R}_2, ..., \mathbf{R}_{n_b}) \in \mathbb{R}^{3Nn_b}$, where we use the compact notation $\mathbf{R}_k = (\mathbf{r}_1^k, \mathbf{r}_2^k, ..., \mathbf{r}_N^k) \in \mathbb{R}^{3N}$. \mathbf{R}_k contains the vector position of all the beads that belong to replica $k \in \{1, 2, ..., n_b\}$. Similarly, we denote $\mathbf{P} = (\mathbf{P}_1, \mathbf{P}_2, ..., \mathbf{P}_{n_b}) \in \mathbb{R}^{3Nn_b}$, where $\mathbf{P}_k = (\mathbf{p}_1^k, \mathbf{p}_2^k, ..., \mathbf{p}_N^k) \in \mathbb{R}^{3N}$ and $\mathbf{p}_i^k \in \mathbb{R}^3$ is the momentum of bead k of ring-polymer i.

The canonical partition function of the classical ringpolymer system (with distinguishable ring-polymers and beads) is given by

$$Z_{n_b}(N, V, T) = \frac{1}{h^{3Nn_b}} \int_V \prod_{i=1}^N d\mathbf{r}_i^1 \cdots d\mathbf{r}_i^{n_b} \int_{-\infty}^{\infty} \prod_{i=1}^N d\mathbf{p}_i^1 \cdots d\mathbf{p}_i^{n_b}$$
$$\times \exp(-\beta \mathcal{H}_{RP}(\mathbf{R}, \mathbf{P}))$$
(28)

where $\beta = 1/k_BT$ (k_B is the Boltzmann's constant) and

$$\mathcal{H}_{RP}(\mathbf{R}, \mathbf{P}) = \sum_{i=1}^{N} \sum_{k=1}^{n_b} \frac{(\mathbf{p}_i^k)^2}{2m_i} + \sum_{i=1}^{N} \sum_{k=1}^{n_b} \frac{1}{2} k_{sp} (\mathbf{r}_i^{k+1} - \mathbf{r}_i^k)^2 + \frac{1}{n_b} \sum_{k=1}^{n_b} U(\mathbf{r}_1^k, \mathbf{r}_2^k ..., \mathbf{r}_N^k)$$
(29)

is the Hamiltonian of the ring-polymer system; k_{sp} is the spring constant of the ring-polymers. $U(\mathbf{r}_1^k, \mathbf{r}_2^k, \dots, \mathbf{r}_N^k)$ is the potential energy of replica k and, hence, U defines the interactions among the kth beads of the different ring-polymers. Note that in eq 29 and throughout this section, $\mathbf{r}_i^{n_b+1} = \mathbf{r}_i^1$ for $i \in \{1, 2, ..., N\}$ (i.e., the polymers are *ring*-polymers). It follows from eq 29 that the potential energy of the ring-polymer system (and hence, the RP-PEL) is given by

$$U_{RP}(\mathbf{R}) = \sum_{i=1}^{N} \sum_{k=1}^{n_b} \frac{1}{2} k_{sp} (\mathbf{r}_i^{k+1} - \mathbf{r}_i^k)^2 + \frac{1}{n_b} \sum_{k=1}^{n_b} U(\mathbf{r}_1^k, \mathbf{r}_2^k, ..., \mathbf{r}_N^k)$$
(30)

The Hessian at an IS

The Hessian of the ring-polymer system is a $(3Nn_b \times 3Nn_b)$ -square matrix with elements given by

$$[\mathbf{H}^{RP}]_{i,k,\alpha}^{j,l,\beta} = \frac{\partial^2 U_{RP}}{\partial r_{i,\alpha}^k \partial r_{j,\beta}^l} \tag{31}$$

z}. We order the elements of the Hessian matrix so that, along any given row, all coordinates with the same value of k (replica number) are grouped together, with $k = 1, 2, ..., n_h$ increasing from left to right [see Figure 10a]. Moreover, within the sequence of (consecutive) elements in the Hessian matrix with a given value of k, we group together all the coordinates with same value of i, with i = 1, 2, ..., N increasing from left to right [Figure 10a]. For given values of i and k, there are only three elements, differing by the corresponding value of $\alpha = x$, y, z. These three elements are ordered so $\alpha = x$, y, z, from left to right [Figure 10a]. A similar ordering of the Hessian elements is used for any given column with indices (j, l, β) [see Figure 10b]. As shown in Figure 10c, the resulting Hessian matrix has a simple structure. Specifically, the Hessian matrix is a square block-matrix composed of $(n_b \times n_b)$ blocks [see Figure 10c]. Each block is a square $3N \times 3N$ -submatrix that can be located within the Hessian matrix by the indices (k, l), with k = 1, 2, ... n_b increasing from left to right, and $l = 1, 2, ..., n_b$ increasing from top to bottom.

It follows from eq 31 that the Hessian matrix is symmetric; as we show below, most blocks in the Hessian matrix are equal to the null matrix [see eq 32 below].

The first-order derivatives of the ring-polymers potential energy (eq 30) are given by

$$\begin{split} \frac{\partial U_{RP}}{\partial r_{i,\alpha}^{k}} &= k_{sp}(2r_{i,\alpha}^{k} - r_{i,\alpha}^{k+1} - r_{i,\alpha}^{k-1}) \\ &+ \frac{1}{n_{b}} \frac{\partial U(r_{1,x}^{k}, r_{1,y}^{k}, r_{1,z}^{k}; \dots; r_{N,x}^{k}, r_{N,y}^{k}, r_{N,z}^{k})}{\partial r_{i,\alpha}^{k}} \end{split}$$

It follows from this expression that the Hessian elements are given by

$$\begin{aligned} [\mathbf{H}^{RP}]_{i,k,\alpha}^{j,l,\beta} &= \frac{\partial^{2} U_{RP}}{\partial r_{i,\alpha}^{k} \partial r_{j,\beta}^{l}} \\ &= k_{sp} (2\delta_{i,k,\alpha}^{j,l,\beta} - \delta_{i,k+1,\alpha}^{j,l,\beta} - \delta_{i,k-1,\alpha}^{j,l,\beta}) \\ &+ \frac{1}{n_{b}} \delta_{k}^{l} \frac{\partial^{2} U(r_{1,x}^{k}, r_{1,y}^{k}, r_{1,z}^{k}; ...; r_{N,x}^{k}, r_{N,y}^{k}, r_{N,z}^{k})}{\partial r_{i,\alpha}^{k} \partial r_{j,\beta}^{l}} \end{aligned}$$
(32)

where $\delta_{i,k,\alpha}^{j,l,\beta}=1$ if i=j and k=l and $\alpha=\beta;$ $\delta_{i,k,\alpha}^{j,l,\beta}=0$, otherwise. The last term of eq 32 has a very simple interpretation. Specifically, let's consider a classical system of N atoms with a potential energy given by $U(r_{1,x^j}, r_{1,y^j}, r_{1,z}; ...; r_{N,x^j}, r_{N,y^j}, r_{N,z})$ where $(r_{1,x^j}, r_{1,y^j}, r_{1,z}; ...; r_{N,x^j}, r_{N,y^j}, r_{N,z})$ are the atoms coordinates. The function U(...) defines the PEL of such an atomic system, which we will refer to as the classical PEL (CL-PEL). The last term of eq 32 is nothing else but the Hessian matrix of the N-atoms system evaluated at point $R_k = (r_{1,x^j}^k, r_{1,z^j}^k, ...; r_{N,x^j}^k, r_{N,y^j}^k, r_{N,z}^k)$ of the CL-PEL, i.e.,

$$[\mathbf{H}^{CL}(\mathbf{R}_k)]_{i,\alpha}^{j,\beta} = \frac{\partial^2 U(r_{1,x}^k, r_{1,y}^k, r_{1,z}^k; ...; r_{N,x}^k, r_{N,y}^k, r_{N,z}^k)}{\partial r_{i,\alpha}^k \partial r_{i,\beta}^l}$$

It follows that

$$[\mathbf{H}^{\text{RP}}]_{i,k,\alpha}^{j,l,\beta} = k_{sp} (2\delta_k^l - \delta_{k+1}^l - \delta_{k-1}^l) \delta_{i\alpha}^{j\beta} + \frac{1}{n_h} \delta_k^l [\mathbf{H}^{\text{CL}}(\mathbf{R}_k)]_{i,\alpha}^{j,\beta}$$
(33)

i.e., the Hessian of the ring-polymer system at the configuration given by R depends solely on the ring-polymers springs (first term of eq 33) and on the Hessian matrix of the classical atomic system evaluated at the replica configurations R_1 , R_2 ,, and R_{n_h} (second term of eq 33).

Equation 33 implies that, consistent with Figure 10c, the Hessian matrix of the ring-polymer system is a block matrix, specifically,

$$\mathbf{H}^{RP}(\mathbf{R}) = \begin{pmatrix} 2k_{sp}\mathbf{1} + \frac{\mathbf{H}^{CL}(\mathbf{R}_{1})}{n_{b}} & -k_{sp}\mathbf{1} & -k_{sp}\mathbf{1} \\ -k_{sp}\mathbf{1} & 2k_{sp}\mathbf{1} + \frac{\mathbf{H}^{CL}(\mathbf{R}_{2})}{n_{b}} & -k_{sp}\mathbf{1} \\ & -k_{sp}\mathbf{1} & \ddots & \ddots & \\ & & \ddots & 2k_{sp}\mathbf{1} + \frac{\mathbf{H}^{CL}(\mathbf{R}_{n_{b}-1})}{n_{b}} & -k_{sp}\mathbf{1} \\ & -k_{sp}\mathbf{1} & 2k_{sp}\mathbf{1} + \frac{\mathbf{H}^{CL}(\mathbf{R}_{n_{b}})}{n_{b}} \end{pmatrix}$$
(34)

where each block is a $(3N \times 3N)$ matrix. In eq 34, only the non-zero block matrices are included; 1 is the identity matrix of $(3N \times 3N)$ -dimensions.

Eigenvectors and Eigenvalues of the Hessian Matrix

We rewrite the Hessian matrix of the ring-polymer system, eq 34, as

$$\mathbf{H}^{RP}(\mathbf{R}) = -k_{sp} \begin{pmatrix} (-2)\mathbf{1} & \mathbf{1} & & & \mathbf{1} \\ \mathbf{1} & (-2)\mathbf{1} & \mathbf{1} & & & \\ & \mathbf{1} & \ddots & \ddots & & \\ & & \ddots & (-2)\mathbf{1} & \mathbf{1} \\ \mathbf{1} & & \mathbf{1} & (-2)\mathbf{1} \end{pmatrix}$$

$$+ \frac{1}{n_{b}} \begin{pmatrix} \mathbf{H}^{CL}(\mathbf{R}_{IS}) & & & \\ & \ddots & & & \\ & & \mathbf{H}^{CL}(\mathbf{R}_{IS}) & & \\ & & \ddots & & \\ & & & \mathbf{H}^{CL}(\mathbf{R}_{IS}) \end{pmatrix}$$

$$(35)$$

where we substituted $\mathbf{R}_1 = \mathbf{R}_2 = ... = \mathbf{R}_{n_b} = \mathbf{R}_{IS}$ since all ring-polymers are assumed to be collapsed at the IS.

Equation 35 implies that the Hessian matrix is the sum of two terms, where each term is the tensor product of two matrices (linear maps). Specifically,

$$\mathbf{H}^{RP}(\mathbf{R}_{IS}) = -k_{sp}\mathbf{T}_{n_b} \otimes \mathbf{1} + \frac{1}{n_b}\mathbf{1}_{n_b} \otimes \mathbf{H}^{CL}(\mathbf{R}_{IS})$$
(36)

where **1** and $\mathbf{H}^{CL}(\mathbf{R}_{IS})$ are $(3N \times 3N)$ -square matrices, and $\mathbf{1}_{n_b}$ are $(n_b \times n_b)$ -square matrices. **1** and $\mathbf{1}_{n_b}$ are the identity matrices and

$$\mathbf{T}_{n_b} = \begin{pmatrix} -2 & 1 & & & 1\\ 1 & -2 & 1 & & & \\ & \ddots & \ddots & \ddots & & \\ & & 1 & -2 & 1\\ 1 & & & 1 & -2 \end{pmatrix}$$
(37)

It follows from eq 36 that $\mathbf{H}^{RP}(\mathbf{R}_{IS})$ is the representation of a linear operator acting on the tensor product $U \otimes V$ of the

vector spaces $U = \mathbb{R}^{n_b}$ and $V = \mathbb{R}^{3N}$, i.e., $\mathbf{H}^{RP}(\mathbf{R}_{IS}) : U \otimes V \rightarrow U \otimes V$.

In order to obtain the eigenvectors/eigenvalues of $\mathbf{H}^{RP}(\mathbf{R}_{IS})$, we start from eq 36 and introduce the eigenvectors/eigenvalues of $\mathbf{H}^{CL}(\mathbf{R}_{IS})$,

$$\mathbf{H}^{\mathrm{CL}}(\mathbf{R}_{\mathrm{IS}})\mathbf{v}_{n} = \lambda_{n}\mathbf{v}_{n} \tag{38}$$

where $\mathbf{v}_n = (v_{n,1} \ v_{n,2} \dots v_{n,3N})^{\mathrm{T}}$ and $n \in \{1, 2, ..., 3N\}$. The 3N pairs $(\omega_n^0 \equiv \sqrt{\lambda_n}, \mathbf{v}_n)$ have an important physical meaning; they represent the vibrational frequencies and normal modes of the classical N-atoms system when it oscillates about the IS of the CL-PEL given by \mathbf{R}_{IS} .

We also introduce the eigenvectors/eigenvalues of $T_{n,\nu}$

$$\mathbf{T}_{n_b}\mathbf{u}_m = \eta_m \mathbf{u}_m \tag{39}$$

where $\mathbf{u}_m = (\mathbf{u}_{m,1} \ u_{m,2} \ ... \ u_{m,n_b})^{\mathrm{T}}$ and $m \in \{1, 2, ..., n_b\}$. It can be shown by direct substitution that the eigenvalues of \mathbf{T}_{n_b} are $\eta_m = -2 + 2 \cos\left(\frac{2\pi}{n_b}m\right)$ with $m = 1, 2, ..., n_b$. If n_b is even, the corresponding orthonormal eigenvectors \mathbf{u}_m are defined by the following vector components,

$$u_{m,n} = \sqrt{\frac{1}{n_b}}, \quad m = n_b \tag{40}$$

$$u_{m,n} = \sqrt{\frac{2}{n_b}} \cos\left(\frac{2\pi}{n_b}nm\right), \quad m = 1, ..., n_b/2 - 1$$
 (41)

$$u_{n_b-m,n} = \sqrt{\frac{2}{n_b}} \sin\left(\frac{2\pi}{n_b}nm\right), \quad m = 1, ..., n_b/2 - 1$$
 (42)

$$u_{m,n} = (-1)^n, \quad m = n_b/2$$
 (43)

where $n = 1, 2, ..., n_b$. If n_b is odd, the vector components of \mathbf{u}_m are also given by eqs 40-43 but with the following modifications: (i) $m = 1, ..., (n_b - 1)/2$ in eqs 41 and 42, and (ii) eq 43 is removed.

Next, we show that the vectors

$$\mathbf{w}_{m,n} = \mathbf{u}_{m} \otimes \mathbf{v}_{n} = \begin{pmatrix} u_{m,1} \mathbf{v}_{n} \\ u_{m,1} \mathbf{v}_{n,2} \\ \vdots \\ u_{m,1} \mathbf{v}_{n,3N} \end{pmatrix} = \begin{pmatrix} u_{m,2} \mathbf{v}_{n,1} \\ u_{m,2} \mathbf{v}_{n,2} \\ \vdots \\ u_{m,2} \mathbf{v}_{n,3N} \end{pmatrix} = \begin{pmatrix} u_{m,2} \mathbf{v}_{n,1} \\ u_{m,2} \mathbf{v}_{n,2} \\ \vdots \\ u_{m,2} \mathbf{v}_{n,3N} \end{pmatrix} = \begin{pmatrix} u_{m,2} \mathbf{v}_{n,1} \\ u_{m,2} \mathbf{v}_{n,2} \\ \vdots \\ \vdots \\ u_{m,n_{b}} \mathbf{v}_{n,1} \\ u_{m,n_{b}} \mathbf{v}_{n,2} \\ \vdots \\ u_{m,n_{b}} \mathbf{v}_{n,2} \end{pmatrix}$$

$$(44)$$

with $m \in \{1, 2, ..., n_b\}$ and $n \in \{1, 2, ..., 3N\}$ are $3Nn_b$ eigenvectors of $\mathbf{H}^{RP}(\mathbf{R}_{IS})$ with corresponding eigenvalues $\gamma_{m,n} = -k_{\rm sp}\eta_m + \frac{1}{n_b}\lambda_n$.

Using eq 36, one can write

$$\mathbf{H}^{RP}(\mathbf{R}_{IS})\mathbf{w}_{m,n} = \mathbf{H}^{RP}(\mathbf{R}_{IS})(\mathbf{u}_m \otimes \mathbf{v}_n)$$

$$= \left(-k_{sp}\mathbf{T}_{n_b} \otimes \mathbf{1} + \frac{1}{n_b}\mathbf{1}_{n_b} \otimes \mathbf{H}^{CL}(\mathbf{R}_{IS})\right)(\mathbf{u}_m \otimes \mathbf{v}_n)$$
(45)

Since

$$(\mathbf{T}_{n} \otimes \mathbf{1})(\mathbf{u}_{m} \otimes \mathbf{v}_{n}) = \mathbf{T}_{n} \mathbf{u}_{m} \otimes \mathbf{1} \mathbf{v}_{n} = \eta_{m} (\mathbf{u}_{m} \otimes \mathbf{v}_{n})$$

and

$$(\mathbf{1}_{n_b} \otimes \mathbf{H}^{CL}(\mathbf{R}_{IS}))(\mathbf{u}_m \otimes \mathbf{v}_n) = \mathbf{1}_{n_b} \mathbf{u}_m \otimes \mathbf{H}^{CL}(\mathbf{R}_{IS}) \mathbf{v}_n$$
$$= \lambda_n (\mathbf{u}_m \otimes \mathbf{v}_n)$$

it follows from eq 46 that

$$\mathbf{H}^{RP}(\mathbf{R}_{IS})\mathbf{w}_{m,n} = \left(-k_{sp}\eta_m + \frac{1}{n_b}\lambda_n\right)\mathbf{w}_{m,n}$$
(47)

In other words, the vector $\mathbf{w}_{m,n}$ is an eigenvector of $\mathbf{H}^{RP}(\mathbf{R}_{IS})$ with eigenvalues $\gamma_{m,n} = -k_{sp}\eta_m + \frac{1}{n}\lambda_n$.

Alternative (Brute Force) Method to Obtain the Eigenvectors/Eigenvalues of the Hessian Matrix

The eigenvectors/eigenvalues of $\mathbf{H}^{RP}(\mathbf{R}_{IS})$ can also be obtained from eq 35 by working with block matrices. To do so, we evaluate separately the effect of each of the two matrices of eq 35 on the vector $\mathbf{w}_{m,n}$.

(i) Using eq 44 for $\mathbf{w}_{m,n}$ one can write

$$\begin{pmatrix}
\mathbf{H}^{\mathrm{CL}}(\mathbf{R}_{IS}) & & & \\
& \ddots & & \\
& \mathbf{H}^{\mathrm{CL}}(\mathbf{R}_{IS}) & & \\
& & \ddots & \\
& & \mathbf{H}^{\mathrm{CL}}(\mathbf{R}_{IS})
\end{pmatrix}$$

$$= \begin{pmatrix}
u_{m,1}\mathbf{H}^{\mathrm{CL}}(\mathbf{R}_{IS})\mathbf{v}_{n} \\
u_{m,2}\mathbf{H}^{\mathrm{CL}}(\mathbf{R}_{IS})\mathbf{v}_{n} \\
\vdots \\
u_{m,n_{b}}\mathbf{H}^{\mathrm{CL}}(\mathbf{R}_{IS})\mathbf{v}_{n}
\end{pmatrix}$$

$$= \lambda_{n} \begin{pmatrix}
u_{m,1}\mathbf{v}_{n} \\
u_{m,2}\mathbf{v}_{n} \\
\vdots \\
u_{m,n_{b}}\mathbf{v}_{n}
\end{pmatrix}$$

$$\vdots \\
u_{m,n_{b}}\mathbf{v}_{n}$$
(48)

where we made use of eq 38.

(ii) Similarly,

$$\begin{pmatrix}
(-2)\mathbf{1} & \mathbf{1} & \mathbf{1} \\
\mathbf{1} & (-2)\mathbf{1} & \mathbf{1} \\
& \ddots & \ddots & \ddots \\
& \mathbf{1} & (-2)\mathbf{1} & \mathbf{1} \\
\mathbf{1} & \mathbf{1} & (-2)\mathbf{1}
\end{pmatrix}
\begin{pmatrix}
u_{m,1}\mathbf{v}_{n} \\
u_{m,2}\mathbf{v}_{n} \\
\vdots \\
u_{m,n_{b}}\mathbf{v}_{n}
\end{pmatrix}$$

$$= \begin{pmatrix}
(-2u_{m,1} + u_{m,2} + u_{m,n_{b}})\mathbf{v}_{n} \\
(u_{m,1} - 2u_{m,2} + u_{m,3})\mathbf{v}_{n} \\
(u_{m,2} - 2u_{m,3} + u_{m,4})\mathbf{v}_{n} \\
\vdots \\
(u_{m,n_{b}-2} - 2u_{m,n_{b}-1} + u_{m,n_{b}})\mathbf{v}_{n} \\
(u_{m,1} + u_{m,n_{b}-1} - 2u_{m,n_{b}})\mathbf{v}_{n}
\end{pmatrix}$$
(49)

However, it follows from eqs 37 and 39 that

$$\begin{cases} -2u_{m,1} + u_{m,2} + u_{m,n_b} = \eta_n u_{m,1} \\ u_{m,1} - 2u_{m,2} + u_{m,3} = \eta_n u_{m,2} \\ u_{m,2} - 2u_{m,3} + u_{m,4} = \eta_n u_{m,3} \\ \vdots \\ u_{m,n_b-2} - 2u_{m,n_b-1} + u_{m,n_b} = \eta_n u_{m,n_b-1} \\ u_{m,1} + u_{m,n_b-1} - 2u_{m,n_b} = \eta_n u_{m,n_b} \end{cases}$$

and, hence,

$$\begin{pmatrix}
(-2)\mathbf{1} & \mathbf{1} & & \mathbf{1} \\
\mathbf{1} & (-2)\mathbf{1} & \mathbf{1} & & \\
& \ddots & \ddots & \ddots & \\
& & \mathbf{1} & (-2)\mathbf{1} & \mathbf{1} \\
\mathbf{1} & & & \mathbf{1} & (-2)\mathbf{1}
\end{pmatrix}
\begin{pmatrix}
u_{m,1}\mathbf{v}_{n} \\ u_{m,2}\mathbf{v}_{n} \\ \vdots \\ u_{m,n_{b}}\mathbf{v}_{n}
\end{pmatrix} = \eta_{n} \begin{pmatrix}
u_{m,1}\mathbf{v}_{n} \\ u_{m,2}\mathbf{v}_{n} \\ \vdots \\ u_{m,n_{b}}\mathbf{v}_{n}
\end{pmatrix}$$
(50)

Therefore, using eqs 48, 50, and 35, one can recover the final result, eq 47.

Physical Interpretation

Summarizing, we found that if (i) the ring-polymer system is at an IS of the RP-PEL, and (ii) all ring-polymers are collapsed

into a single point (i.e., $\mathbf{R}_1 = \mathbf{R}_2 = ... = \mathbf{R}_{n_b} \equiv \mathbf{R}_{IS}$), then the eigenvalues of the ring-polymer hessian matrix $\mathbf{H}^{RP}(\mathbf{R}_{IS})$ are given by,

$$\gamma_{m,n} = -k_{sp} \left(-2 + 2 \cos \left(\frac{2\pi}{n_b} m \right) \right) + \frac{1}{n_b} \lambda_n \tag{51}$$

where $m=1, 2, ..., n_b$ and n=1, 2, ..., 3N. Importantly, the 3N values $\{\lambda_n\}$ are the eigenvalues of $\mathbf{H}^{\mathrm{CL}}(\mathbf{R}_{\mathrm{IS}})$. This means that every vibrational mode with frequency $\omega_n^{\mathrm{CL}} = \sqrt{\lambda_n}$ of the N-atom system (when it is at the IS of the CL-PEL given by \mathbf{R}_{IS}) generates n_b vibrational modes for the ring-polymer system with frequencies $\omega_{m,n}^{\mathrm{RP}} = \sqrt{\gamma_{m,n}}$.

The eigenvectors $\mathbf{w}_{m,n}$ of $\mathbf{H}^{RP}(\mathbf{R}_{IS})$, associated with the eigenvalues $\gamma_{m,n}$, are given by eq 44. These eigenvectors define the normal modes of vibration of the ring-polymer system. The first 3N components of $\mathbf{w}_{m,n}$ define the normal mode components of the beads belonging to replica 1, the next 3N components of $\mathbf{w}_{m,n}$ define the normal mode components of the beads belonging to replica 2, and so on.

An interesting conclusion follows from eq 51. In the case where $m=n_b$, eq 51 indicates that $\gamma_{m=n_b,n}=\frac{1}{n_b}\lambda_n$; i.e., the ring-polymers' normal modes have the same frequencies as the N-atoms system but re-scaled by the factor $\frac{1}{\sqrt{n_b}}$, i.e., $\omega_{n_b,n}^{RP}=\frac{1}{\sqrt{n_b}}\omega_n^{CL}$. The corresponding eigenvectors can be written in a simple form (see eqs 40 and 44),

$$\mathbf{w}_{m=n_b,n} = \frac{1}{\sqrt{n_b}} \begin{pmatrix} \mathbf{v}_n \\ \mathbf{v}_n \\ \vdots \\ \mathbf{v}_n \end{pmatrix}$$
(52)

Therefore, in the ring-polymer normal modes with $m=n_b$ (and n=1, 2, ..., 3N), the normal mode components of all the replicas are identical, and given by \mathbf{v}_n . In other words, all ring-polymers remain collapsed and oscillate as a single atom. Moreover, the normal mode $(m=n_b, n)$ of the collapsed ring-polymers is the same as the normal mode n of the classical N-atom system, re-scaled by the factor $\frac{1}{\sqrt{n_b}}$ (eq 52).

ASSOCIATED CONTENT

5 Supporting Information

The Supporting Information is available free of charge at https://pubs.acs.org/doi/10.1021/acs.jctc.3c01085.

(i) Effects of varying the number of beads per ring polymer (n_b) on our results, (ii) proof of eq 19, based on the HA of the PEL, and (iii) further tests of the HA for the RP-PEL based on heating PIMC simulations (PDF)

AUTHOR INFORMATION

Corresponding Authors

Yang Zhou — Department of Physics, Brooklyn College of the City University of New York, Brooklyn, New York 11210, United States; Ph.D. Program in Physics, The Graduate Center of the City University of New York, New York, New York 10016, United States; ⊙ orcid.org/0000-0002-0142-1507; Email: yzhou4@gradcenter.cuny.edu

Gustavo E. Lopez — Department of Chemistry, Lehman College of the City University of New York, Bronx, New York 10468, United States; Ph.D. Program in Chemistry, The Graduate Center of the City University of New York, New York, New York 10016, United States; orcid.org/0000-0003-1660-547X; Email: gustavo.lopez1@ lehman.cuny.edu

Nicolas Giovambattista — Department of Physics, Brooklyn College of the City University of New York, Brooklyn, New York 11210, United States; Ph.D. Program in Physics, The Graduate Center of the City University of New York, New York, New York 10016, United States; Ph.D. Program in Chemistry, The Graduate Center of the City University of New York, New York, New York 10016, United States; orcid.org/0000-0003-1149-0693;

Email: ngiovambattista@brooklyn.cuny.edu

Complete contact information is available at: https://pubs.acs.org/10.1021/acs.jctc.3c01085

Notes

The authors declare no competing financial interest.

ACKNOWLEDGMENTS

This work was supported by the SCORE Program of the National Institutes of Health under award number 1SC3GM139673 and the NSF CREST Center for Interface Design and Engineered Assembly of Low Dimensional Systems (IDEALS), NSF Grant Number HRD-1547830. This work was also supported, in part, by a grant of computer time from the City University of New York High-Performance Computing Center under NSF Grants CNS-0855217, CNS-0958379, and ALI-1126113.

REFERENCES

- (1) Kauzmann, W. The Nature of the Glassy State and the Behavior of Liquids at Low Temperatures. *Chem. Rev.* **1948**, 43, 219–256.
- (2) Angell, C. A.; Ngai, K. L.; McKenna, G. B.; McMillan, P. F.; Martin, S. W. Relaxation in Glass-Forming Liquids and Amorphous Solids. *J. Appl. Phys.* **2000**, *88*, 3113–3157.
- (3) Binder, K.; Kob, W. Glassy Materials and Disordered Solids: An Introduction to Their Statistical Mechanics, Rev. Ed.; World Scientific: Hackensack, NJ; London; Singapore, 2011.
- (4) Ediger, M. D.; Harrowell, P. Perspective: Supercooled Liquids and Glasses. J. Chem. Phys. 2012, 137, No. 080901.
- (5) Stillinger, F. H.; Debenedetti, P. G. Glass Transition Thermodynamics and Kinetics. Annu. Rev. *Condens. Matter Phys.* **2013**, *4*, 263–285.
- (6) Berthier, L.; Ediger, M. D. Facets of Glass Physics. *Phys. Today* 2016, 69, 40-46.
- (7) Berthier, L.; Biroli, G. Theoretical Perspective on the Glass Transition and Amorphous Materials. *Rev. Mod. Phys.* **2011**, 83, 587.
- (8) Tarjus, G.; Kivelson, S. A.; Nussinov, Z.; Viot, P. The Frustration-Based Approach of Supercooled Liquids and the Glass Transition: A Review and Critical Assessment. *J. Phys.: Condens. Matter* **2005**, *17*, R1143–R1182.
- (9) Chandler, D.; Garrahan, J. P. Dynamics on the Way to Forming Glass: Bubbles in Space-Time. *Annu. Rev. Phys. Chem.* **2010**, *61*, 191.
- (10) Stillinger, F. H. Energy Landscapes, Inherent Structures, and Condensed-Matter Phenomena; Princeton University Press: Princeton, 2016.
- (11) Adam, G.; Gibbs, J. H. On the Temperature Dependence of Cooperative Relaxation Properties in Glass-Forming Liquids. *J. Chem. Phys.* **1965**, 43, 139–146.
- (12) Niu, H.; Yang, Y.; Jensen, S.; Holzmann, M.; Pierleoni, C.; Ceperley, D. M. Stable Solid Molecular Hydrogen Above 900 K from

- Machine-Learned Potential Trained with Diffusion Quantum Monte Carlo. *Phys. Rev. Lett.* **2023**, *130*, No. 076102.
- (13) Kinugawa, K.; Takemoto, A. Quantum Polyamorphism in Compressed Distinguishable Helium-4. *J. Chem. Phys.* **2021**, *154*, No. 224503.
- (14) Eltareb, A.; Lopez, G. E.; Giovambattista, N. The Importance of Nuclear Quantum Effects on the Thermodynamic and Structural Properties of Low-Density Amorphous Ice: A Comparison with Hexagonal Ice. *J. Phys. Chem. B* **2023**, *127*, 4633–4645.
- (15) Goldstein, M. Viscous Liquids and the Glass Transition: A Potential Energy Barrier Picture. J. Chem. Phys. 1969, 51, 3728.
- (16) Stillinger, F. H.; Weber, T. A. Hidden Structure in Liquids. *Phys. Rev. A* **1982**, 25, 978.
- (17) Stillinger, F. H.; Weber, T. A. Packing Structures and Transitions in Liquids and Solids. *Science* **1984**, 225, 983.
- (18) Debenedetti, P. G.; Truskett, T. M.; Lewis, C. P.; Stillinger, F. H. Theory of Supercooled Liquids and Glasses: Energy Landscape and Statistical Mechanics. *Adv. Chem. Eng.* **2001**, *28*, 21.
- (19) Sastry, S. Inherent Structure Approach to the Study of Glass-Forming Liquids. *Phase Transitions* **2002**, *75*, 507–517.
- (20) Sciortino, F. Potential Energy Landscape Description of Supercooled Liquids and Glasses. *J. Stat. Mech.* **2005**, 2005, No. P05015.
- (21) Heuer, A. Exploring the Potential Energy Landscape of Glass-Forming Systems: From Inherent Structures via Metabasins to Macroscopic Transport. *J. Phys.: Condens. Matter* **2008**, 20, No. 373101.
- (22) Giovambattista, N.; Lopez, G. E. Potential Energy Landscape Formalism for Quantum Liquids. *Phys. Rev. Research* **2020**, 2, No. 043441.
- (23) Wales, D. J. Exploring Energy Landscapes. Annu. Rev. Phys. Chem. 2018, 69, 401–25.
- (24) Stillinger, F. H. Inherent Structure Formalism for Quantum Liquids. J. Chem. Phys. 1988, 89, 4180.
- (25) Saika-Voivod, I.; Sciortino, F.; Poole, P. H. Free Energy and Configurational Entropy of Liquid Silica: Fragile-to-Strong Crossover and Polyamorphism. *Phys. Rev. E* **2004**, *69*, No. 041503.
- (26) Handle, P. H.; Sciortino, F. Potential Energy Landscape of TIP4P/2005 Water. *J. Chem. Phys.* **2018**, *148* (13), No. 134505.
- (27) Sun, G.; Xu, L.; Giovambattista, N. Relationship between the Potential Energy Landscape and the Dynamic Crossover in a Waterlike Monatomic Liquid with a Liquid-Liquid Phase Transition. *J. Chem. Phys.* **2017**, *146* (1), No. 014503.
- (28) Allen, M. P.; Tildesley, D. J. Computer Simulation of Liquids, 2nd ed.; Oxford University Press: Oxford, UK, 2017.
- (29) Kim, K. H.; Amann-Winkel, K.; Giovambattista, N.; Späh, A.; Perakis, F.; Pathak, H.; Parada, M. L.; Yang, C.; Mariedahl, D.; Eklund, T.; Lane, T. J.; You, S.; Jeong, S.; Weston, M.; Lee, J. H.; Eom, I.; Kim, M.; Park, J.; Chun, S. H.; Poole, P. H.; Nilsson, A. Experimental Observation of the Liquid-Liquid Transition in Bulk Supercooled Water under Pressure. *Science* **2020**, *370* (6519), 978–982.
- (30) Abraham, J. Y.; Buldyrev, S. V.; Giovambattista, N. Liquid and Glass Polymorphism in a Monatomic System with Isotropic, Smooth Pair Interactions. *J. Phys. Chem. B* **2011**, *115* (48), 14229–14239.
- (31) Nguyen, B.; Lopez, G. E.; Giovambattista, N. Nuclear Quantum Effects on the Liquid-Liquid Phase Transition of a Water-Like Monatomic Liquid. *Phys. Chem. Chem. Phys.* **2018**, *20*, 8210.
- (32) Liu, Y.; Sun, G.; Eltareb, A.; Lopez, G. E.; Giovambattista, N.; Xu, L. Nuclear Quantum Effects on the Thermodynamic Response Functions of a Polymorphic Waterlike Monatomic Liquid. *Phys. Rev. Res.* 2020, 2, No. 013153.
- (33) Eltareb, A.; Lopez, G. E.; Giovambattista, N. Nuclear Quantum Effects on the Dynamics and Glass Behavior of a Monatomic Liquid with Two Liquid States. *J. Chem. Phys.* **2022**, *156*, No. 204502.
- (34) Press, W. H. Numerical Recipes: The Art of Scientific Computing, 3rd ed.; Cambridge University Press: Cambridge, UK; New York, 2007.

- (35) Tuckerman, M. Statistical Mechanics and Molecular Simulations; Oxford University Press: Oxford, UK, 2008.
- (36) Bernu, B.; Ceperley, D. M. Path Integral Monte Carlo. In *Quantum Simulations of Complex Many-Body Systems: From Theory to Algorithms, Lecture Notes*; Grotendorst, J., Marx, D., Muramatsu, A., Eds.; John von Neumann Institute for Computing: Jülich, 2002; NIC Series, Vol. 10, ISBN 3-00-009057-6, pp 51–61.
- (37) Sciortino, F.; Kob, W.; Tartaglia, P. Inherent Structure Entropy of Supercooled Liquids. *Phys. Rev. Lett.* **1999**, *83* (16), 3214–3217.
- (38) Altabet, Y. E.; Stillinger, F. H.; Debenedetti, P. G. A Cavitation Transition in the Energy Landscape of Simple Cohesive Liquids and Glasses. *J. Chem. Phys.* **2016**, *145* (21), No. 211905.
- (39) Altabet, Y. E.; Fenley, A. L.; Stillinger, F. H.; Debenedetti, P. G. Cavitation Transition in the Energy Landscape: Distinct Tensile Yielding Behavior in Strongly and Weakly Attractive Systems. *J. Chem. Phys.* **2018**, *148* (11), No. 114501.
- (40) Zhou, Y.; Lopez, G. E.; Giovambattista, N. Anomalous Properties in the Potential Energy Landscape of a Monatomic Liquid Across the Liquid-Gas and Liquid-Liquid Phase Transitions. *J. Chem. Phys.* **2022**, *157*, No. 124502.
- (41) Sastry, S. The Relationship between Fragility, Configurational Entropy and the Potential Energy Landscape of Glass-Forming Liquids. *Nature* **2001**, *409* (6817), 164–167.
- (42) Richardson, J. O. Ring-Polymer Approaches to Instanton Theory, Thesis Dissertation; Pembroke College, University of Cambridge, 2012.
- (43) Siebrand, W.; Smedarchina, Z.; Zgierski, M. Z.; Fernandez-Ramos, A. Proton Tunnelling in Polyatomic Molecules: A Direct Dynamics Instanton Approach. *Int. Rev. Phys. Chem.* **1999**, *18*, 5.
- (44) Mil'nikov, G. V.; Nakamura, H. Practical Implementation of the Instanton Theory for the Ground-State Tunneling Splitting. *J. Chem. Phys.* **2001**, *115*, 6881.
- (45) Richardson, J. O.; Althorpe, S. C. Ring-Polymer Instanton Method for Calculating Tunneling Splittings. *J. Chem. Phys.* **2011**, 134, No. 054109.
- (46) To show this, we consider the case where (i) the ring-polymer system is at an IS of the RP-PEL with all the ring-polymers collapsed, $\mathbf{R}_1 = \mathbf{R}_2 = ... = \mathbf{R}_{n_b} = \mathbf{R}_{IS}^{CL}$, and where (ii) \mathbf{R}_{IS}^{CL} is an IS of the CL-PEL. Note that point (ii) implies that \mathbf{R}_k is the local minimum of $U(\mathbf{R})$ for all replicas $k=1,2,...,n_b$. Now, the RP-PEL is defined by eq 5. The first term of this expression is at a minimum under condition (i) since this term is initially zero and increases if any bead is displaced. Similarly, the second term is also initially at a minimum due to point (ii). Accordingly, the total potential energy of the ring-polymer system $\mathcal{U}_{\mathrm{RP}}$ is a minimum under assumptions (i) and (ii), and hence, the ring-polymer system is at an IS of the RP-PEL with all ring-polymers being collapsed.
- (47) Scala, A.; Starr, F. W.; La Nave, E.; Sciortino, F.; Stanley, H. E. Configurational Entropy and Diffusivity of Supercooled Water. *Nature* **2000**, 406 (6792), 166–169.
- (48) Sastry, S.; Debenedetti, P. G.; Stillinger, F. H. Signatures of Distinct Dynamical Regimes in the Energy Landscape of a Glass-Forming Liquid. *Nature* **1998**, 393, 554.

Supplementary Information for "The Harmonic and Gaussian Approximations in the Potential Energy Landscape Formalism for Quantum Liquids"

Yang Zhou 1,2,* , Gustavo E. Lopez 3,4,* , and Nicolas Giovambattista 1,2,4,**

¹ Department of Physics, Brooklyn College of the City University of New York, Brooklyn, New York 11210, United States

² Ph.D. Program in Physics,

The Graduate Center of the City University of New York, New York, NY 10016, United
States

³ Department of Chemistry, Lehman College of the City University of New York, Bronx, New York 10468, United States

⁴ Ph.D. Program in Chemistry,

The Graduate Center of the City University of New York, New York, NY 10016, United
States

E-mail: yzhou4@gradcenter.cuny.edu,gustavo.lopez1@lehman.cuny.edu,ngiovambattista@brooklyn.cuny.edu

1 Results from PIMC simulations Using Different Number of Beads per Ring-Polymer

Fig. S1(a) shows the total energy of the quantum Fermi-Jagla (QFJ) liquids E(T) from PIMC simulations with Planck's constant $h = h_3$. Included are the values of E(T) reported in Fig. 2(a) of the main manuscript for a system composed of N = 1000 atoms/ring-polymers and for the case of $n_b = 10$ beads per ring-polymer. Also included are the results from PIMC simulations for (a) $(N = 512, n_b = 10)$, and $(N = 512, n_b = 20)$. Fig. S1(b) and S1(c) are, respectively, the inherent structures (IS) energy $E_{IS}(T)$ and vibrational energy $E_{vib}(T)$ corresponding to the simulations included in Fig. S1(a). Briefly, the values of E(T), $E_{IS}(T)$, and $E_{vib}(T)$ practically overlap for the cases $(N = 512, n_b = 10)$ and $(N = 1000, n_b = 10)$ suggesting that our results are not affected by system size effects (N). This applies to the temperatures at which the system is in equilibrium (empty symbols) and out-of-equilibrium (solid symbols).

A comparison of the values of E(T), $E_{IS}(T)$, and $E_{vib}(T)$ for the cases $(N = 512, n_b = 10)$ and $(N = 512, n_b = 20)$ show that, in the equilibrium liquid state at $T \ge 0.09$ $(h = h_3)$, our results in the main manuscript for the case $n_b = 10$ practically converged with respect to n_b . However, small deviations remain in the equilibrium liquid state at T = 0.06 - 0.09 and at lower temperatures, in the out-of-equilibrium states studied. For the smaller values of $h = h_1$, h_2 , our results converged with $n_b = 10$ (see Ref.¹).

2 Ring-polymer Collapse at the IS

Fig. S2(a) shows the radius of gyration $R_g(T)$ as a function of temperature associated with the QFJ liquids at v = 2.2 and Planck's constants $h = h_1$, h_2 , h_3 . Triangles are the $R_g(T)$ calculated from the instantaneous configurations; circles, are the values of $R_g(T)$ at the corresponding IS. For all the values of h studied, we find that the ring-polymers are spread at all temperatures studied; $R_g(T) > 0$ and increases upon cooling in the equilibrium liquid states (empty triangles). However, at the corresponding IS, the ring-polymers collapse. Indeed, at the IS and for all temperatures where the system is in equilibrium (empty circles), $R_g(T) = 0$. We note that in Fig. S2(a) $R_g > 0$ for the IS obtained at $T \le 0.02$ and $h = h_2, h_3$; a larger values of n_b at these conditions lead to $R_g = 0$ (see Ref. 1).

The results shown in Fig. S2(a) are general and valid to volumes that expand from the liquid-to-vapor spinodal, $v \approx 5.0-6.0$ to the very high-density liquid state, $v \approx 1.0.^3$ To show this, included in Fig. S2(b) is the radius of gyration $R_g(T)$ as a function of volume associated with the QFJ liquids for the Planck's constants $h = h_1$, h_2 , h_3 . The results for $h = h_1$, h_2 , h_3 are for T = 0.13, 0.09, 0.05, respectively (in the three cases, T = 0.83 T_c where T_c is the liquid-liquid critical point temperature of the corresponding QFJ liquid²). Fig. S2(b) shows that for all the values of h and volumes studied, $R_g(v) > 0$ in the instantaneous configurations (triangles), i.e., the ring-polymers are expanded. Instead, the ring-polymers are collapsed $R_g = 0$ at the corresponding IS.

3 Normal Modes Vibrational Frequencies of the Ring-Polymer System

In the main manuscript, it is shown that Eq. 25 predicts remarkably well the vibrational frequencies associated with the normal modes of the ring-polymer system. The tests in the main manuscript are performed for $n_b = 10$; see Figs. 3 and 4. In Fig. S3 we include additional results obtained with different numbers of beads and atoms/ring-polymers. The predictions from Eq. 25 are in agreement with our PIMC simulations.

4 Vibrational Free Energy with the Harmonic Approximation of the PEL

In this section, we evaluate the vibrational Helmholtz free energy of the ring-polymer system, $F_{vib}(N, V, T)$, within the harmonic approximation (HA) of the RP-PEL. Eq. 12 of the main manuscript gives the the free energy of the system in the imaginary situation where the system is only allowed to visit IS with energy e_{IS} ,

$$F_{vib}(N, V, T; e_{IS}) \equiv -k_B T \ln \left(\langle Q_l(N, V, T) \rangle_{e_{IS}} \right) \tag{1}$$

Here, $\langle ... \rangle_{e_{IS}}$ represents an average over all basins with IS energy e_{IS} , and we assume that all atoms have the same mass. In equilibrium, $e_{IS} \to E_{IS}(N, V, T)$ and hence, $F_{vib}(N, V, T) = F_{vib}(N, V, T; e_{IS} = E_{IS})$. In Eq. 1, $Q_l(N, V, T)$ is the canonical partition function of basin l (when the reference value for the potential energy of the system is set to zero at the corresponding IS), and is given by Eq. 9 of the main manuscript; specifically,

$$Q_l(N, V, T) = \frac{1}{h^{3n_b N}} \int_{-\infty}^{\infty} e^{-\beta \sum_{i=1}^{N} \sum_{k=1}^{n_b} \frac{(\mathbf{p}_i^k)^2}{2m'}} dp^{3n_b N} \int_{V_l} e^{-\beta \Delta \mathcal{U}_l} dr^{3n_b N}$$
(2)

In the HA,⁴ the potential energy about the IS of basin l is approximated by a quadratic function (i.e, the first non-zero term of the Taylor expansion of ΔU_l about the corresponding IS),

$$\Delta \mathcal{U}_{l} \approx \frac{1}{2} \sum_{i,j=1}^{N} \sum_{k,n=1}^{n_{b}} \sum_{\alpha,\beta=1}^{3} \left(\frac{\partial^{2} \mathcal{U}_{l}}{\partial r_{i,\alpha}^{k} \partial r_{j,\beta}^{n}} \right)_{at\ IS} (r_{i,\alpha}^{k} - r_{i,\alpha}^{k,IS}) (r_{j,\beta}^{n} - r_{j,\beta}^{n,IS})$$
(3)

where $\{r_{i,\alpha}^k\}$ are the coordinates of bead $k=1,2...n_b$ of ring-polymer i=1,2...N, component $\alpha=x,y,z$, and $\{r_{i,\alpha}^{k,IS}\}$ are the corresponding coordinates at the IS of basin l.

By introducing a set of $3n_bN$ generalized coordinates $\{q_j\}_{j=1,2...,3n_bN}$ (normal mode coordinates), it is possible to rewrite Eq. 3 as a sum of $3n_bN$ independent harmonic oscillators

with frequency $\{\omega_j\}_{j=1,2...,3n_bN}$,⁵

$$\Delta \mathcal{U}_l \approx \frac{1}{2} \sum_{j=1}^{3n_b N} m' \omega_j^2 q_j^2 \tag{4}$$

The term $m\omega_j^2$ is the spring constant associated to the harmonic oscillator j. The $3n_bN$ values $\{m'\omega_j^2\}$ are the eigenvalues of the Hessian matrix,

$$H_{i,k,\alpha}^{j,n,\beta} = \left(\frac{\partial^2 \mathcal{U}_l}{\partial r_{i,\alpha}^k \partial r_{j,\beta}^n}\right)_{at\ IS} \tag{5}$$

Using the generalized coordinates $\{q_j\}$, Eq. 2 can be expressed in terms of Gaussian distributions,

$$Q_l(N, V, T) = \frac{1}{h^{3n_b N}} \int_{-\infty}^{\infty} e^{-\beta \sum_{j=1}^{3Nn_b} \frac{p_j^2}{2m^l}} dp^{3n_b N} \int_{V_l} e^{-\beta/2 \sum_{i=1}^{3n_b N} m\omega_j^2 q_j^2} dq^{3Nn_b}$$
 (6)

Since at sufficient low temperatures one may approximate $\int_{V_l} ...dq^{3n_bN} \to \int_{-\infty}^{\infty} ...dq^{3n_bN}$, Eq. 6 can be solved,⁴ leading to the expression

$$Q_l(N, V, T) = \prod_{j=1}^{3n_b N} (\beta \hbar \omega_j)^{-1}$$
(7)

It follows that the vibrational free energy of the system within the HA of the PEL is given by

$$F_{vib}(N, V, T) = k_B T \ln \left(\left\langle \prod_{j=1}^{3n_b N} (\beta \hbar \omega_j) \right\rangle_{E_{IS}} \right)$$
 (8)

where, again, $\langle ... \rangle_{E_{IS}}$ represents an average over all basins with IS energy $e_{IS} = E_{IS}(N, V, T)$. For classical systems composed on N atoms, the following approximation is commonly used in the literature (see, e.g., Ref.⁷)

$$\ln\left(\left\langle \prod_{j=1}^{3N} (\beta \hbar \omega_j) \right\rangle \right) \approx \left\langle \ln\left(\prod_{j=1}^{3N} (\beta \hbar \omega_j)\right) \right\rangle \tag{9}$$

which usually introduces an error smaller than 1%.⁶ Using Eq. 9 (with $N \to n_b N$), the vibrational Helmholtz free energy is given by⁷

$$F_{vib}(N, V, T) \approx 3N n_b k_B T \ln \left(\beta \hbar \omega_0\right) + k_B T \mathcal{S}(N, V, T; E_{IS}) \tag{10}$$

where ω_0 is an arbitrary constant with the same units as ω_j , and

$$S(N, V, T; E_{IS}) \equiv \left\langle \ln \left(\prod_{j=1}^{3n_b N} (\omega_j / \omega_0) \right) \right\rangle_{E_{IS}}$$
(11)

is the so-called basin shape function (Eq. 20 of the main manuscript).

5 Harmonic Approximation of the PEL: Heating Runs starting from IS

Here, we perform additional tests of the harmonic approximation of the PEL for the QFJ liquids/ring-polymer systems studied. Specifically, we perform out-of-equilibrium PIMC simulations where we heat configurations of the system from T=0 up to T>0.10 (at which the system may reach equilibrium). The starting configurations of the system are IS obtained from the equilibrium liquid at a temperature T_0 (v=2.2). The expectation is that during the heating runs, at least for very low temperatures, the system will remain in a single basin of the PEL. Accordingly, upon heating at very low temperatures, one should observe that the total energy of the system is given by $E(T) = E_{IS}^0 + E_{vib}(T)$, where E_{IS}^0 is the (constant) IS energy of the basin where the system is trapped, and $E_{vib}(T)$ is given

by Eq. 26 of the main manuscript (harmonic approximation). During the heating runs, we perform PIMC simulations at T = 0.005, 0.010, 0.015, 0.020, 0.040, ...0.20, sequentially. At each T, PIMC simulations are performed for 2000 simulation steps and 100 IS are calculated every 20 PIMC steps.

Fig. S4 shows the total energy E(T), IS energy $E_{IS}(T)$, and vibrational energy of the QFJ liquid $E_{vib}(T) = E(T) - E_{IS}(T)$ during the out-of-equilibrium heating runs. For each value of the Planck's constant h, we consider two values of T_0 ; results for $h = h_3$ are for $T_0 = 0.06$, 0.08 while results for $h = h_1$, h_2 are for $T_0 = 0.10$, 0.14. The results are summarized as follows.

- (i) For the case $h = h_1$, Fig. S4(c) shows that the harmonic approximation (Eq. 26) holds up to $\approx 0.16 0.20$. This is a large temperature considering that the system leaves the basin of the RP-PEL, where it is initially located, at approximately T > 0.10. Indeed, $E_{IS}(T)$ remains constant only for approximately T < 0.10 (blue lines in Fig. S4(b)).
- (ii) The cases $h = h_2$, h_3 are complicated by the fact that E_{IS} is not constant at very low temperatures. Specifically, in these cases, E_{IS} decreases slightly upon heating at T < 0.020, suggesting that the starting basin may be very shallow and hence, the system can move to nearby basins of the RP-PEL. Nonetheless, Fig. S4(c) shows that the harmonic approximation (Eq. 26) holds up to $\approx 0.04 0.06$. We note that if the basins explored by the system at T < 0.04 0.06 are similar, i.e., have a similar shape function, then Eq. 26 is expected to hold as well.

References

- (1) Giovambattista, N.; Lopez, G. E. Potential Energy Landscape Formalism for Quantum Liquids. *Phys. Rev. Research* **2020**, 2, 043441.
- (2) Nguyen, B.; Lopez, G. E.; Giovambattista, N. Nuclear Quantum Effects on the Liquid-

- Liquid Phase Transition of a Water-Like Monatomic Liquid. *Phys. Chem. Chem. Phys.* **2018**, 20, 8210.
- (3) Zhou, Y.; Lopez, G. E.; Giovambattista, N. Anomalous Properties in the Potential Energy Landscape of a Monatomic Liquid Across the Liquid-Gas and Liquid-Liquid Phase Transitions. J. Chem. Phys. 2022, 157, 124502.
- (4) Stillinger, F. H. Energy Landscapes, Inherent Structures, and Condensed-Matter Phenomena. Princeton University Press: Princeton, 2016.
- (5) Goldstein, H. Classical Mechanics, 2nd Ed.; Addison-Wesley: 1980.
- (6) La Nave, E.; Mossa, S.; Sciortino, F. Potential Energy Landscape Equation of State. *Phys. Rev. Lett.* **2002**, 88 (22), 225701.
- (7) Sciortino, F. Potential Energy Landscape Description of Supercooled Liquids and Glasses. J. Stat. Mech. 2005, P05015.

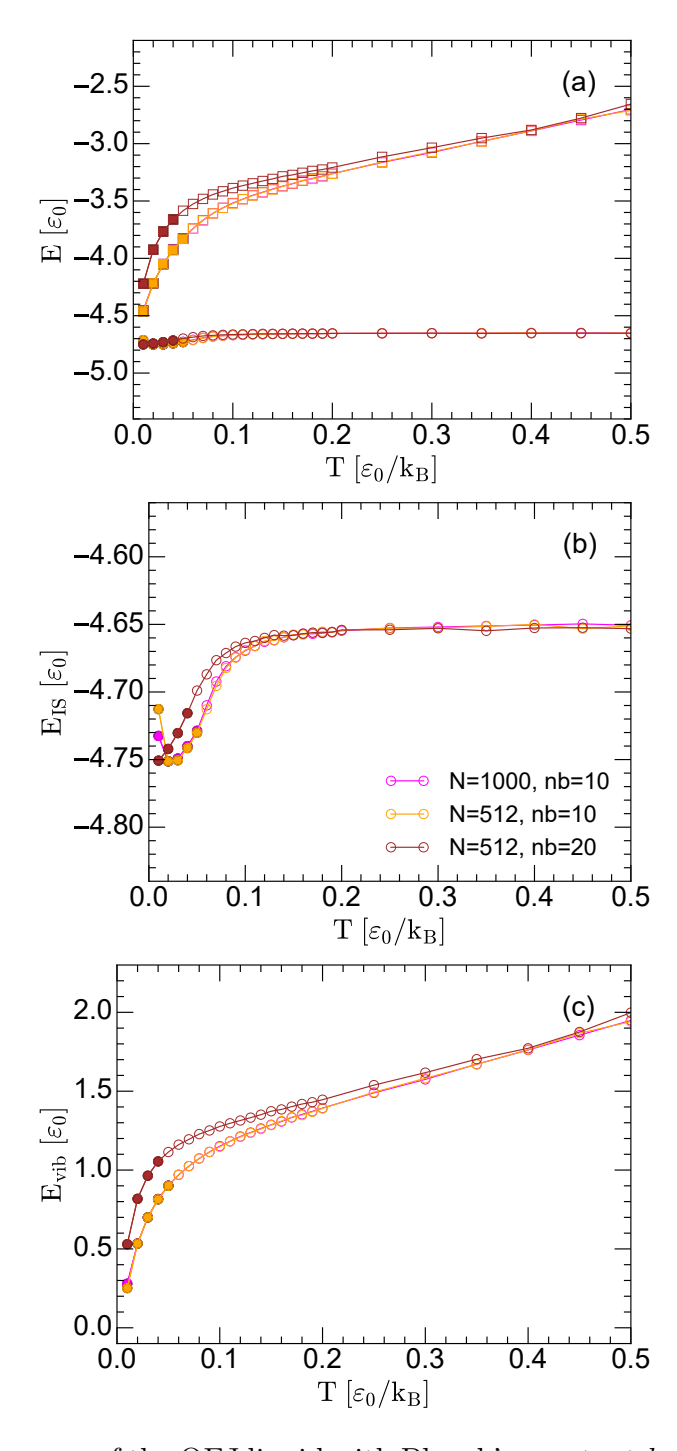


Figure S1: (a) Total energy of the QFJ liquid with Planck's constant $h=h_3$, and for different number of atoms N and beads per ring-polymer n_b (v=2.2). For comparison, also included are the corresponding IS energy of the system. (b) IS energy and (c) vibrational energy of the ring-polymer system from the PIMC simulations included in (a). All energies are given per atom (divided by N). Empty and solid symbols indicate equilibrium liquid and out-of-equilibrium states, respectively.

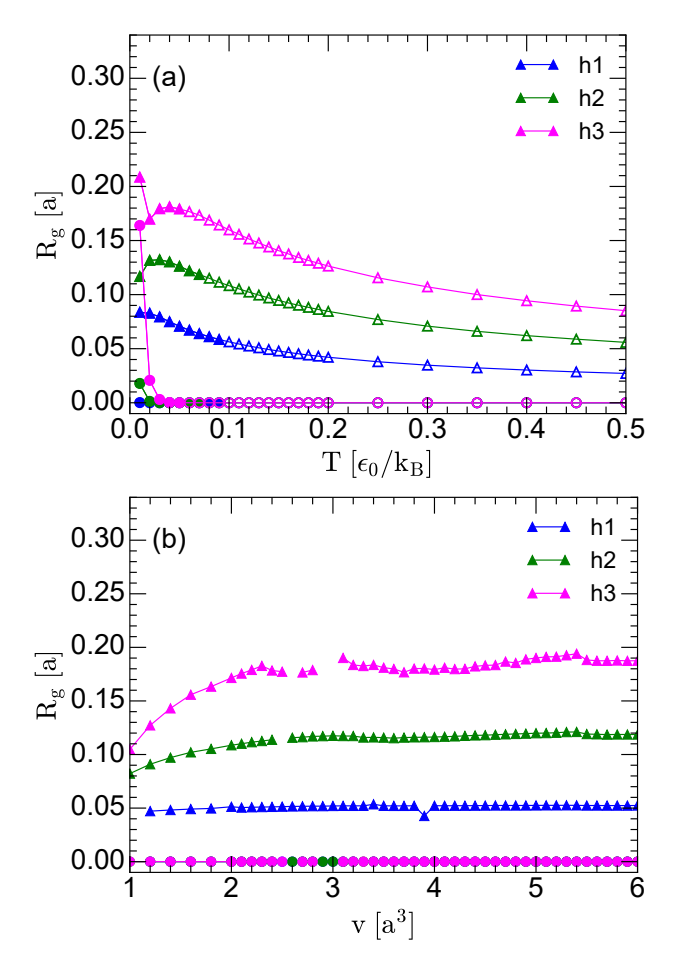


Figure S2: (a) Radius of gyration $R_g(T)$ as a function of temperature associated with the atoms of the QFJ liquids at v=2.2 and Planck's constants $h=h_1,\ h_2,\ h_3$. Triangles are the $R_g(T)$ calculated from the instantaneous configurations; circles, are the values of $R_g(T)$ at the corresponding IS. Empty and solid symbols correspond to the equilibrium liquid and out-of-equilibrium states, respectively. (b) Same as (a) for the case of PIMC simulations performed at different volumes and T=x0.13 $(h=h_1),\ T=0.09$ $(h=h_2),\$ and T=0.05 $(h=h_3).$ In all cases, the ring-polymers are expanded in the liquid state $(R_g>0)$ but collapse at the corresponding IS $(R_g=0)$.

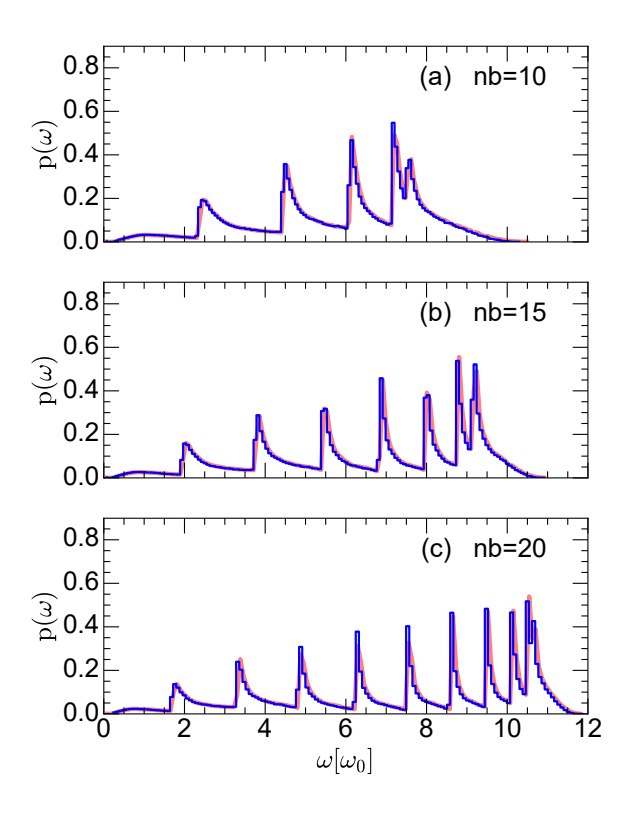


Figure S3: Distribution of IS normal mode frequencies $P(\omega)$ of the ring-polymer system systems associated to the QFJ liquids with Planck's constant $h=h_3$. Results are for systems with N=512 atoms/ring-polymers and $n_b=10,15,20$ beads per ring-polymer; T=0.15 and v=2.2. Magenta lines correspond to the frequencies obtained numerically, by calculating the eigenvalues of the Hessian matrix of the ring-polymer systems; blue lines are the frequencies given by Eq. 25 of the main manuscript.

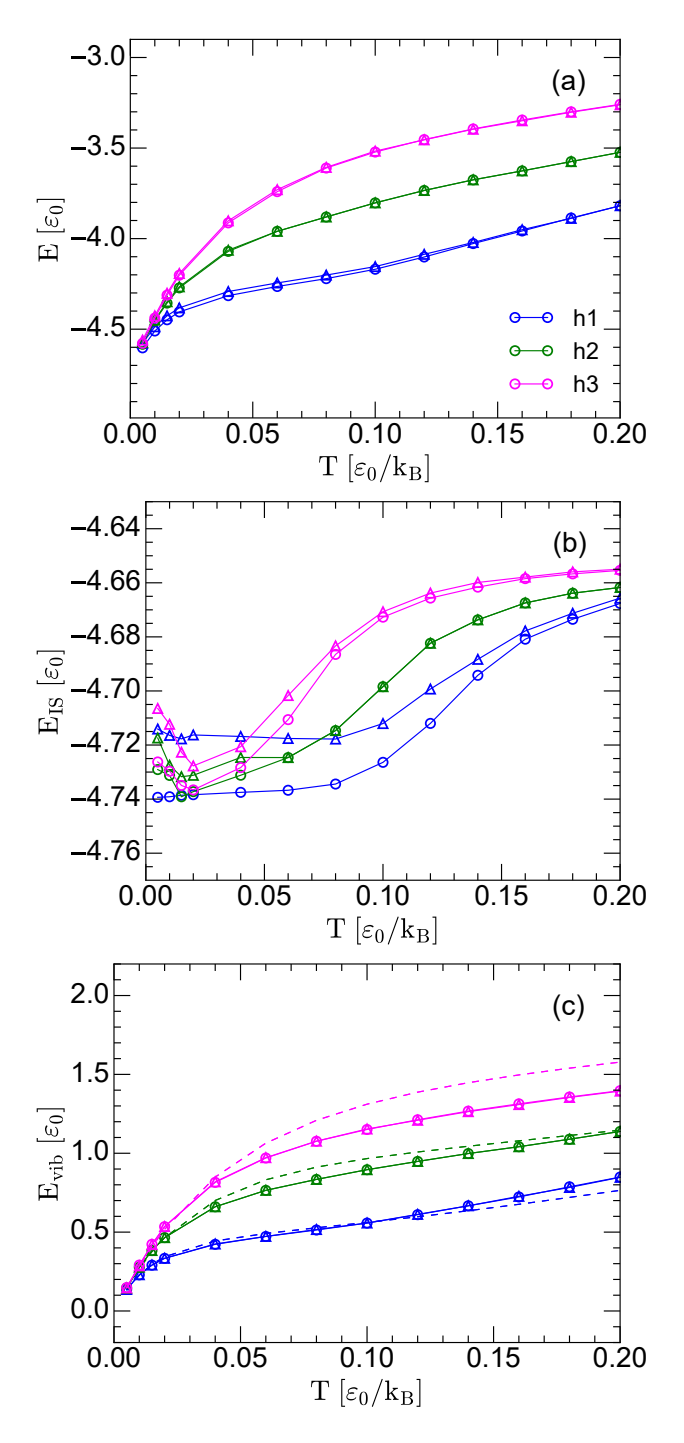


Figure S4: (a) Total energy E(T) and (b) IS energy $E_{IS}(T)$ (per particle) during out-of-equilibrium heating runs at v = 2.2. The starting configurations at T = 0 are IS taken from equilibrium runs at temperature T_0 (v = 2.2). Results for $h = h_3$ are for $T_0 = 0.06$ (circles), 0.08 (triangles); results for $h = h_2$ are for $T_0 = 0.08$ (circles), 0.10 (triangles); results for $h = h_1$ are for $T_0 = 0.10$ (circles), 0.14 (triangles) [for each T_0 and t_0 , all properties are averaged over five independent runs]. (c) Vibrational energy, $E_{vib}(T) = E(T) - E_{IS}(T)$, extracted from (a) and (b). The dashed line is the $E_{vib}(T)$ predicted by Eq. 26 of the main manuscript based on the harmonic approximation of the RP-PEL. In all cases, and at low temperatures, the behavior of $E_{vib}(T)$ is fully consistent with the harmonic approximation of the RP-PEL.

12